Discovering gravitational waves with Advanced LIGO

Jess McIver[a] and D.H. Shoemaker[b]

[a]The University of British Columbia, Vancouver, BC V6T 1Z4, Canada; [b]LIGO Laboratory, Kavli Institute for Astrophysics and Space Research, Massachusetts Institute of Technology, 185 Albany St, Cambridge, MA 02139, USA

ARTICLE HISTORY
Compiled June 1, 2021

ABSTRACT
Gravitational-wave astronomy started in earnest in 2015 with the first observation of waves from a binary black hole merger by NSF's LIGO detectors. Since that time, the signals from many colliding compact objects have been observed with LIGO and Virgo, giving insights into the demographics of stellar black holes, the nature of neutron stars and the products of their coalescence. Detailed studies of the signals are in agreement with the predictions of General Relativity. The instruments which enabled these measurements are of extraordinary sensitivity, and the treatment of the data to enable the observational science requires a deep understanding of the instruments and best practices for analysis. The field is rich with future opportunities to participate in this broad swath of science.

1. Introduction

On September 14, 2015, gravitational waves generated more than 1300 million years in the past reached the Earth. The two gravitational wave detectors of the National Science Foundation's Laser Interferometer Gravitational-Wave Observatory (LIGO) recorded the stretching and squeezing of space as the wave passed the first detector, and then seven thousandths of a second later, the second detector. From the signature of these signals it was possible to infer the distance to the source, and establish that it must have been due to two black holes 36 and 29 times the mass of the Sun which coalesced to form a single larger black hole. This astonishing observation [1] marked the start of a new field of observational gravitational-wave astronomy.

The direct observation of gravitational waves was a further confirmation of Einstein's theory of general relativity (GR). It also launched the use of gravitational waves (GWs) as a tool to explore the Universe, taking advantage of some unique features of this new messenger. Detectable GW signals are generated by the motion of star-scale masses, in contrast to electromagnetic (EM) emission like light and radio waves, which are emitted by the acceleration of subatomic-scale particles. GWs are very weakly interacting, and are effectively not scattered or blocked by intervening matter, unlike light and radio waves. Also, GW detectors sense the amplitude of the signal, rather than the power, so that the detected signal falls linearly in strength as $1/r$ rather than as $1/r^2$ for many astronomical telescopes, allowing a cosmological reach.

mciver@phas.ubc.ca

Gravitational waves (GW) travel at the speed of light, and like radio or light waves affect matter perpendicular to the direction of propagation. In contrast to light, however, gravitational waves (GW) traveling along e.g., the z axis affect space-time itself, and introduce a strain in space, squeezing then stretching along the x axis while stretching then squeezing along the y axis.

GW signals, even from tens of solar masses swinging around each other at nearly the speed of light, are minuscule. This is due in part to the fact that there is just one gravitational 'charge' (unlike the positive and negative charges of atomic particles which generate light), making the generation of signals less efficient. In addition, space-time is 'stiff' – it is hard to distort spacetime. The consequence is that GW detectors must be extraordinarily sensitive to the effects of passing GWs, able to see changes of the order of one part in 10^{20} in the geometry of space. To try to gain perspective, this is a fractional resolution equivalent to sensing (in 1/100 of a second!) a change in distance to the nearest star, Alpha Centuri, of just the thickness of a piece of paper.

This article is an introduction to anew field using Advanced LIGO as an example. Advanced LIGO is the second generation of gravitational wave detectors installed in the US LIGO Observatories, and the first instruments to have the required sensitivity to made a direct detection of GWs. We present the basic concepts of generation and detection of GWs, along with methods to gain confidence in a GW signal. This article can serve as a point of departure for further reading and participation in gravitational-wave astrophysics. We hope to convey our excitement about the future of all aspects of this field – the astrophysics, the data analysis, and the evolution of the detector technology.

2. History

Gravitational waves first started to be seriously considered in the early 1900's with the advent of a solid understanding of electromagnetism and the propagation of electrical signals at the speed of light and with an effect transverse to the direction of propagation. Einstein took up the question of the compatibility of gravitational waves (GWs) with his (1915) general theory of relativity (GR), having found that a linearized form of his equations had wave solutions, leading to papers in 1916 and 1918 [2] on the topic. This latter paper first proposed that there should be GWs consistent with GR. In fact, Einstein's understanding of GWs changed over the years, with papers both supporting and denying their existence in GR. It was not until 1956 that Pirani was able to resolve a number of theoretical concerns and confusions. In 1957, at a pivotal meeting at Chapel Hill [3], he presented a convincing argument that GWs should carry energy – and thus could be, in principle, detected. We sketch out a brief history of the field in Figure 1.

In the 1960's, Weber, a participant in that meeting and a formidable experimenter, started to pursue the notion of a GW detector based on the longitudinal excitation of a bar of metal. After some refinement, he built a number of these 'bar' detectors consisting of aluminum cylinders, with piezoelectric crystals attached to the side of the cylinder. These piezoelectric crystals develop a voltage when stressed, and thus act as a transducer to convert the longitudinal vibrations of a bar into a voltage. The idea was that an impulsive gravitational wave (from, say, a core-collapse supernova) would pass perpendicular to the axis of the bar, effectively quickly squeezing and stretching it, and so exciting the roughly kilohertz frequency of resonance; this would show up in the voltage across the piezoelectric crystals as though the bar had been hit on one

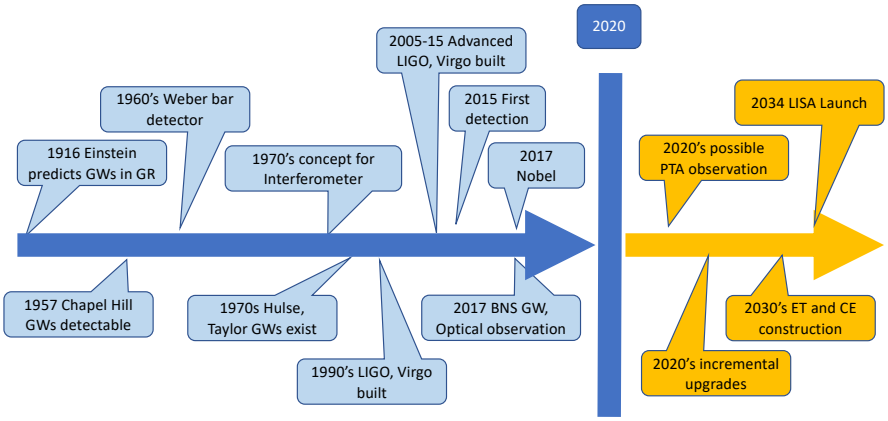

Figure 1. Timeline for the field of gravitational waves. BNS refers to a Binary Neutron Star coalescence. PTA refers to Pulsar Timing Arrays as GW detectors. ET is Einstein Telescope and CE Cosmic Explorer which are planned next-generation observatories. LISA is the Laser Interferometer Space Antenna.

end with a soft hammer. Aluminum has low internal mechanical loss – a bell made of aluminum would ring for a long time. This property should produce a more sensitive detector due to the persistence of the bar response to a transient excitation. The level of excitation would be proportional to the strength of the signal at the bar's resonant frequency, and observing near-simultaneous excitation of widely separated bars could be used to gain confidence that a real signal had been seen. After some initial optimism that signals had been seen, a follow-up effort by a number of groups in the US and Europe in the early 1970's did not did not find any credible signals and thus could not confirm the claimed detection. The technology of bar detectors advanced significantly through the 1990's [4], with great increases in sensitivity brought through cooling of bars to temperatures approaching absolute zero, but no detection of signals was made. It must be stressed that the technologies and the data analysis techniques stimulated by the Weber bars, along with the generated excitement and training of scientists in that domain, was absolutely critical to the future of the field.

In parallel, the radio telescope community was exploring the electromagnetic universe, and Bell and Hewish identified the first *pulsar*, a periodic radio signal from a rotating neutron star in 1967. This was followed in 1974 by Taylor and Hulse's discovery of a pulsar in a system of two neutron stars orbiting around each other (a 'binary'). Through careful observation of the evolution of the orbit – a gradual decrease in the time for one full ∼8-hour orbit – they were able to show that the system was losing energy at just the rate that GR predicted for the energy lost to gravitational waves [5]. This discovery, and other beautiful inferences from this system, earned Hulse and Taylor the 1993 Nobel Prize in Physics. Thus GWs appeared to exist, as inferred from the energy balance in this binary system. However, the direct observation of the amplitude of the wave as a function of time – or 'waveform' – was yet to be seen. Clearly this new astrophysical messenger had the potential to deliver much more new insight on the Universe.

The concept of a GW detector employing optical interferometry as a transducer from strain to voltage was seen independently by a number of scientists as a promising alternative. The first published mention appears to be by Gerstenstein and Pustovoit [6], in a theoretical study from 1963; Weber noted the idea in a lab notebook, and his student Forward also pursued the idea [7]. Weiss, who had been working in the domain

of atomic clocks pursuing applications of the recently-invented laser, fell on the idea quite independently while teaching a course in general relativity. Although it was first presented 'just' as a homework problem, it became clear to Weiss that the concept had a real chance of success if a thorough list of technical challenges he laid out in an internal MIT report [8] could be overcome. He found an early resonance with Isaacson at the US National Science Foundation (NSF), and was able to obtain funding after several attempts to launch development of key technologies. Efforts sprang up in Germany (stimulated by Weiss' efforts), Scotland, and a bit later Caltech, Paris, and Pisa, to refine the technical approaches and to develop more concrete plans for instruments which could reach the required sensitivity for frequent detections. Weiss' 1972 report would effectively serve as a roadmap for a decades-long effort to bring working detectors to fruition. In the US, the remarkable vision and courage of the people at the National Science Foundation to fund the effort has been richly rewarded, and the importance of the initial detection recognized with the award of the 2017 Nobel Prize in Physics to Weiss, with Barry Barish and Kip Thorne. All three stress the importance of the world-wide collaboration to the success of the field.

As we describe in Section 3 below, the strain character of GWs and their incredibly small amplitude means that long arms are needed for realistic detectors. Once it became clear that multi-km arms would be needed, the large scale of a real observatory was evident, and it was obvious that researchers would need to join forces both to solve the technical challenges and to motivate the very significant investments to build observatories. In Europe, German and UK-based researchers developed proposals and ultimately built GEO-600 near Hannover, Germany [9], and French and Italian groups also coalesced to propose and build Virgo near Pisa, Italy [10]. In the US, groups at MIT and Caltech joined to propose in 1989 to the NSF a plan for the Laser Interferometer Gravitational-wave Observatory, or LIGO [11]. This led to the construction of Observatories in Livingston, Louisiana, and Hanford, Washington. Our article will focus on the Advanced LIGO detectors currently installed in LIGO [12], but the world-wide GW effort is central to the success of the field.

Initially, the effort to develop GW detectors had been undertaken by small independent groups and with some sense of competition. The skills of most of the researchers were finely tuned to design, build, and exploit table-top sized experiments. A significant transition was needed to start to look at the engineering challenges of full-scale projects, to divide up responsibilities and eliminate unnecessary parallel efforts, and generally prepare to successfully execute multi-hundred-million-dollar projects. An infusion of approaches, and very skilled persons, from high-energy particle physics was key. In the US, this led to the LIGO Laboratory [13], a joint MIT-Caltech group currently of some 180 persons working to develop and operate the LIGO detectors. There was an additional need to transform the continuously-flowing calibrated data of the detectors into interpretable astrophysical results through data analysis. New communities grew around each of the detectors, notably the Virgo Collaboration [14] and the LIGO Scientific Collaboration (LSC) [15], to address the needs for both continued innovation in the instrumentation and the development of the observational science. The collaborations have grown significantly from their small beginnings, and along the way adopted internal organizations and systems of commitments and rewards which strive to offer opportunities for career growth while carrying out a wide range of scientific and sociological tasks. This coherent effort has been a hallmark of the field, and it would not have succeeded without the community choosing to make commitments to the greater good.

Today, we find collaborations around LIGO, Virgo, and the more recently-built

KAGRA [16] detector in Japan, with some 2000 scientists, students, engineers, technicians, and educators from more than 30 nations directly involved. These three 'LVK' Collaborations now are mature social entities, and have the burdens and opportunities which come with that mantle; work on improving diversity, equity, and inclusion is a growing priority. The instrument science, data, and astrophysical interpretation are shared between the LVK Collaborations to ensure the best science and sociology. The work so far has been richly rewarded and the collaborations are poised to carry the field and its members forward for decades to come.

3. Basic detection mechanism

To gain some intuition for gravitational waves, we can visualize a flat, Minkowski spacetime from special relativity [17] as a stretched rubber sheet. If we add a distribution of mass to this sheet, we'll see some corresponding spacetime curvature and the associated effective gravitational force. If we disturb this distribution of mass, this change in curvature will propagate throughout our rubber spacetime sheet as gravitational waves (we'll see in the next section that an accelerating asymmetric mass distribution is needed). These gravitational waves stretch and squeeze space perpendicular to their direction of travel as they propagate through spacetime at the same fundamental speed limit as light, c. The ultimate goal of a gravitational wave detector is to measure this stretching and squeezing, or *strain* h, as the difference ΔL in length L between two orthogonal directions; $h = \Delta L/L$.

We can achieve this with an experimental setup similar to what Michelson and Morley [18] used to search for a signal of Earth's motion with respect to a theorized 'æther' in 1887. A simple Michelson interferometer as shown in Figure 2, this time using coherent laser light, will allow us to sense spacetime strain by treating the mirrors as *test masses*, freely falling in the x-y plane of the detector and coupled to gravity. Any differences in length between two arms results in a difference in light travel time, and this change in relative phase will be sensed by our output photodiode as a change in light intensity.

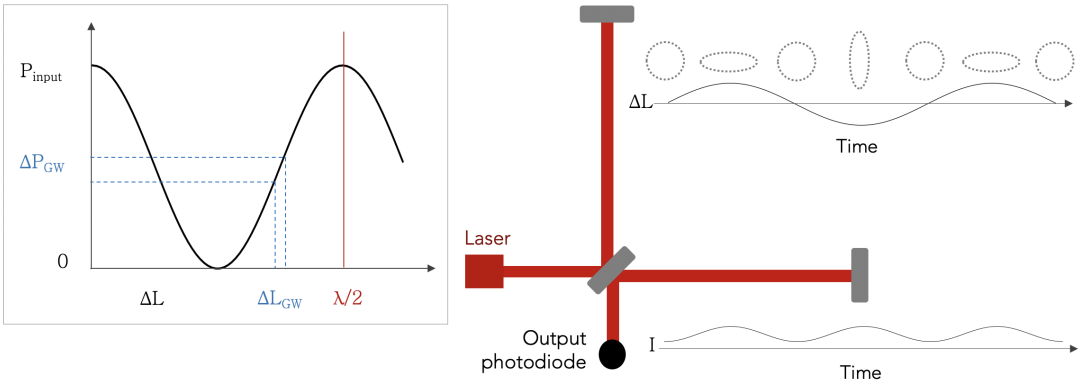

Figure 2. A simple Michelson interferometer. A passing gravitational wave passing through the plane of the detector distorts spacetime as illustrated by the stretched and squeezed circle of test masses (upper right). The difference in length of the two interferometer arms causes a difference in phase in the light traveling in the arms, as described in Equation 1. An output photodiode senses spacetime strain as a change in light intensity over time. The inset shows the intensity at the output varies with arm length difference changes, including how a small differential change in arm length due to a passing GW would induce a small (approximately linear!) change in circulating power.

If we make the path that light travels down an arm in our detector longer, it will accumulate more phase in the presence of a passing gravitational wave, allowing us to more easily differentiate between tiny strain differences in the two arms. We can understand this by relating the expected change in phase, ϕ , due to incident spacetime strain, h, as a function of the length of the arms[1], L, and the wavelength of the laser light, λ:

$$\Delta\phi = 4\pi\frac{Lh}{\lambda} \tag{1}$$

We can then relate power measured at the output photodiode, P_{out}, to this change in phase measured by the detector, $\Delta\phi$, and power input into the interferometer, P_{in} [19]. If we examine the *change* in output power in the linear region of the resulting sinusoid (in between the trough and the crest, where the slope is nearly constant), we can see that P_{out} is approximately linear as a function of Δh, the change in GW strain. This linear region is highlighted with dashed blue lines in the inset of Figure 2.

$$P_{out} = P_{in}\cos^2(\Delta\phi); \qquad \Delta P_{out} = \frac{2\pi L}{\lambda}P_{in}\Delta h \tag{2}$$

In the most straightforward view of a Michelson interferometer, the longer we make our detector arms, the greater the induced phase difference; and the higher the laser power, the bigger the signal. We will see later in Sections 5 and 6 that it is not quite so simple in practice.

A significant feature of this detector is that gravitational waves do not necessarily need to enter the detector from directly overhead for us to sense them. Gravitational waves from almost any direction could produce some difference in phase between the two perpendiular arms in our simple detector (with the exception of the 'corner case' of waves traveling 45° relative to the arms in the plane of the detector, which produce no difference in arm length) [20]; there is no need to be 'pointing in the right direction'. However, our (single) detector's sensitivity to gravitational waves from nearly the entire sky leaves us with little information about their direction of origin.

Unlike telescopes, which can localize sources well by understanding exactly where they are pointing, we require multiple interferometers to localize gravitational wave sources. Similar to triangulating the origin of earthquakes, the relative time of arrival between detectors drives our estimate of the sky location of the source. Using just the time of arrival and two detectors, we can localize roughly to a ring of potential positions, and with three detectors we can narrow that ring down to two likely regions in the sky. We can also make use of what we know about how sensitive our detectors are to gravitational waves as a function of the sky position, or their *antenna pattern*[2] to better estimate likely source position. Our sky localization uncertainties are dominated by estimates of how well we can resolve the time and phase of GWs on arrival, as well as their amplitude, which allows us to directly estimate the distance to the source [22]. Multiple detectors also aid us in establishing confidence in our detections. As we will see in the next section, in practice the Advanced LIGO detectors are susceptible to

[1]Note that this linear relationship between signal strength and detector arm length, L only holds when L is much smaller than the wavelength of an incident GW. We'll see this again in our discussion of future detectors in Section 9.

[2]You can read more about this *antenna pattern* in an excellent living review by Sathyaprakash and Schutz [21], or in Peter Saulson's book on interferometric gravitational wave detection [19]

noise that can mimic or obscure the behavior of a passing gravitational wave.

4. Astrophysics with gravitational waves

4.1. Gravitational wave emission

Now that we have a sense of how gravitational waves interact with our detectors as they pass from our rubber sheet analogy, we'll consider what generates them more quantitatively. To leading order, we can understand the strain h observed by one of our detectors in terms of the gravitational constant, G, the speed of light, c, the distance between the detector and the source, r, and the source's quadrupole moment[3], I.

$$h(t) \propto \frac{G}{c^4}\frac{1}{r}\ddot{I} \tag{3}$$

We see that the generated spacetime strain is proportional to the second time derivative of the system's quadrupole moment denoted $\ddot{I}$ – the acceleration of some asymmetric mass distribution. For example, two point masses orbiting each other will not only have a nonzero I, but also a nonzero $\ddot{I}$. Similarly, a spinning neutron star with some aspherical deformation not aligned with its spin axis would also have a nonzero I and $\ddot{I}$. Equation 3 also highlights a very striking astronomical property of our GW detectors: since we measure h(t), we can have access to unique information about the physics of the source. We also note that telescopes generally sense incident photon power, which decreases as $1/\mathrm{r}^2$. However, our detector is sensitive to gravitational wave *amplitude*, which decreases as $1/r$.

Since general relativity serves as a excellent predictor of the gravitational wave amplitude from the particular source of a 'coalescing binary' – a system of two compact objects over time – we are able to directly measure distance to the source from the time-frequency evolution of the signal. This allows gravitational waves to serve as a complement to light-based methods of estimating distance, such as the standard candle approach, which assumes a known luminosity at a given distance for phenomena like Type Ia supernovae.

Consider also that the constant, G/c^4, is a very small number, on the order of 10^{-45} $\mathrm{s}^2/(\mathrm{kg\ m})$! As most GW sources are very far (millions or billions of light years) from the Earth, the 1/r term is quite small as well. The remaining term $\ddot{I}$ must be *very* large to generate even extremely small fractional changes in length, on the order of 10^{-21}. We'll see that detectable sources are not possible to generate on Earth; these sources are on the same mass scale as stars, and often moving at relativistic speeds.

4.2. Gravitational wave sources

Knowing that the generation of strain is directly connected to an asymmetric acceleration of mass, or the change in quadrupole moment, I_{ij}, over time, we can describe each likely source of gravitational waves for ground-based detectors like Advanced LIGO with this framework of the changing distribution of mass for each system. We'll start with the prototypical Advanced LIGO gravitational-wave signal source: a compact

[3]The quadrupole moment is a tensor, where each element of the tensor is summed over the mass of each system component multiplied by the distance from that component to a coordinate origin in the directions described by that tensor element (i.e. I_{xx} would be the sum over mx^2 for each mass component, and I_{xy} would be the sum over mxy, etc.) A system with perfect spherical symmetry would have zero quadrupole moment.

binary coalescence, or a *CBC*. Indeed, the first gravitational wave signal ever discovered, GW150914, was the coalescence of two stellar-mass black holes detected by the Advanced LIGO instruments in 2015.

If we treat the compact objects in a binary orbit, say neutron stars or black holes, as point sources, then we can model most of their orbital evolution leading up to coalescence very well using general relativity, as the Hulse-Taylor binary system first showed. If we map out the expected waveform of the gravitational radiation from their orbit[4] we will find that spacetime strain is governed by the frequency of their orbit, f, and a quantity known as the *chirp mass*, M_c.

$$h(t) \sim \frac{M_c^{5/3} f^{2/3}}{r} \cos(4\pi f t); \qquad M_c = \frac{(m_1 m_2)^{3/5}}{(m_2 + m_2)^{1/5}} \tag{4}$$

You may notice M_c looks similar to a reduced mass with strange power laws (see [21] for a derivation). M_c is so named because it describes the evolution of the signal as it 'chirps' or sweeps up through the frequency band (upper left of Figure 3). Consistent with our intuition, as the binary system radiates energy in the form of gravitational waves, the binary orbit shrinks, increasing in frequency until coalescence. An interesting feature is that the orbit of the gravitational wave frequency is twice that of the frequency of the orbit (with a bit more general relativity, we will see this is due to the tensor polarization of GWs).

We can also derive a remarkably simple expression to estimate the GW amplitude as a function of the *Schwarzschild radius* r_s of each object, which relates the radius of the event horizon of a simple black hole to its mass: $r_S = 2GM/c^2$. Using Newtonian mechanics, we can relate the frequency of the orbit to the object masses and the radius of their (roughly circular) orbit, R. If we then express the masses in terms of the Schwarzschild radius of each mass (r_{S1} and r_{S2}), we find the GW signal amplitude follows $r_{S1} r_{S2}$ divided by R and and the distance between the CBC and the observer r [19]:

$$|h| \approx \frac{r_{S1} r_{S2}}{R r} \tag{5}$$

For a typical compact binary coalescence signal, this point approximation description will capture the amplitude and most of the evolution of the orbital inspiral, until the compact objects are quite close (i.e. their distance apart is on the same scale as their size). The complex effects of strong field gravity become important to evolution of the quadrupole moment during this 'merger' phase. In the case where one or both of the objects is a neutron star, tidal effects can also introduce additional corrections to the signal waveform. After merger, the final object will 'ring down' like Jell-O© that has been violently struck as non-axisymmetric distortions are radiated away. For these final phases of a coalescence, we need numerical relativity for an accurate description of spacetime strain.

You might have noticed that we have only included black holes and neutron stars in our definition of 'compact' objects. This is because at the sensitive frequency range of the Advanced LIGO detectors (roughly 10-2000 Hz, as we will see later), white dwarfs and larger stars would be tidally pulled apart or otherwise destroyed before

[4] In order to illustrate the basic behavior, Equation 4 also assumes we are only sampling in one direction (unlike our interferometers). The full stretching and squeezing effects are captured in a description of gravitational-wave *polarization*, which you can read more about in [21].

reaching a small enough separation to orbit at a frequency within the LIGO detector sensitivity range. The radius of a typical neutron star is roughly 1000 times smaller than a white dwarf! Those, and many more massive sources inaccessible to the ground-based systems, will be observed by space-based gravitational wave detectors such as LISA [23] that are sensitive to millihertz GW frequencies.

Additionally, pulsar timing arrays [24] will measure correlated differences in the precise pulsing radio signatures of known pulsars to detect the effect of very low frequency (10^{-9} to 10^{-6} Hz) gravitational waves, including the slow inspiral of supermassive black holes in merged galaxies (see [25] for a recent review). Other gravitational-wave experiments aim to detect remnant gravitational waves from the primordial Universe as a polarization signature in the cosmic microwave background.

We expect Advanced LIGO will also be able to observe other sources of gravitational waves. We discuss just a few of them here, and illustrate their observable expected signal duration in Figure 3. For a more complete overview, see [21].

The Advanced LIGO detectors are expected to eventually detect a *stochastic* signal in the form of a superposition of many distant compact object mergers. Each of these mergers would be individually unresolvable by the detectors, but collectively they will sum to produce a random, coherent signal that registers across the detector network. The LVK Collaborations currently expect to see the first hints of this stochastic gravitational wave background with the Advanced LIGO detectors as the detectors evolve and improve to reach design sensitivity. Additionally, there is the potential that GW detectors may also detect gravitational reverberations that are still echoing from the Big Bang. There are a wide variety of models for what the frequency content of such a gravitational wave signal would be, and most are much too small to be observed with the current instruments, but some intersect with the Advanced LIGO detectors' sensitive range of frequencies.

Advanced LIGO is expected to be sensitive to gravitational waves emitted by core-collapse supernova (CCSN) within our own Milky Way galaxy. Modeling these powerful explosions includes a lot of complex interacting physics, including particle physics, electromagnetism, fluid dynamics, and general relativity. Simulations are very computationally expensive, and three dimensional simulations of the most likely explosion mechanism, driven by neutrino interactions, only very recently (within the past 5-10 years) have been able to successfully emulate supernova explosions, like the Crab nebula supernova remnant. As a result, researchers developing models have not yet produced a family of waveforms that has the same level of certainty as binary inspirals. The one galaxy within reach for Advanced LIGO for this source, our own Milky Way, is predicted to produce only one core-collapse supernova per century. Future ground-based gravitational wave detectors with a factor of 10 greater reach will have about a factor of 2 improved chance of registering a CCSN signal as they bring the M81 galaxy into reach [26].

Unlike gravitational wave signals from expected stochastic and supernova sources, the signature of *continuous wave* signals from spinning neutron stars is quite confidently predicted. From radio observations, we know that a significant fraction of neutron stars are spinning quite quickly (tens of times per second for Advanced LIGO sources, or considerably faster) and that their spin speed is very slowly decaying or *spinning down*. If there is some asymmetric feature in a neutron star to create a time-dependent quadrupole moment, say a 'mountain' on the equator caused by the buckling of the crust, then as the star spins, that off-axis asymmetry will produce gravitational waves. We can understand the expected spacetime strain in terms of the characteristic eccentricity of this asymmetric feature, the quadrupole moment of the

spinning star about the spin axis (z), I_z and the frequency of the star's rotation, f: $h(t) \sim \epsilon I_z f^2/r\ cos(4\pi ft)$. Notice that like CBCs, again the gravitational wave signature is emitted at twice the rotational frequency. For known *pulsars* [27], neutron stars that are observed to emit radio pulses as they spin, radio astronomers can measure very precisely where the pulsar is in the sky and how quickly it is spinning as a function of time. Knowing the sky location, f, and the rate-of-change of the frequency $\dot{f}$ enables a near-exact waveform prediction for these galactic pulsars. This has allowed Advanced LIGO and other GW detectors to place interesting constraints on how much of the energy lost in their observed frequency 'spin down' could be accounted for by gravitational waves produced by off-axis asymmetries. You might note that there is much less energy being converted to gravitational waves than for a black hole merger (multiple solar masses of energy are radiated in gravitational waves in less than a second during a black hole merger!). Advanced LIGO is only sensitive to GWs from spinning neutron stars within our galaxy, but already exquisitely so: The equator of the pulsar J0711–6830, located around 358 light years away, is not distorted from a perfect circle by more than the width of a human hair [28].

We summarize the expected GW sources for Advanced LIGO in Figure 3. Depending on the underlying physics, each source will have a characteristic expected duration in the detectors' sensitive frequency range, as well as some degree to which we can model it well. This framework is useful in matching the source we're interested in with the most effective signal processing method to search for it, which we will discuss in the next section. For lower mass CBC systems, including many binary black hole (BBH) systems or especially a binary neutron star (BNS), current waveform models describe the expected signals very accurately for the full range of frequencies accessible to Advanced LIGO. For high mass CBC systems at the edge of Advanced LIGO's low frequency sensitivity, such as an intermediate mass black hole (IMBH) system, relativistic effects become more important in the signal's time-frequency evolution, and the signal has far fewer orbital cycles in the sensitive band of the detectors. Additionally, BBH sources with modulations due to eccentricity (eBBH) and short duration *burst* sources, including core-collapse supernovae (CCSN), are currently not well modeled. The degree that the signal evolution is well-predicted is also a useful distinction for long duration source searches: continuous wave sources are expected to manifest as nearly sinusoidal with well-defined modulations due to the Earth's orbit and rotation, whereas there is not a similar expected pattern for a GW stochastic background. In the next section, we will use these insights to explore optimal methods to search for different types of expected GW signals.

4.3. Searches for gravitational waves

Since we don't expect weakly interacting GW signals to be altered by dust, galaxies, or any other mass between Earth and the source, we can leverage the power of *matched filtering* to compare the detector data directly to well-modeled GW signals. If we compare a template – our best guess for the GW amplitude as a function of time – for one of our expected signals to our detector data, we can calculate the cross correlation between them as the signal-to-noise ratio (SNR). This SNR, ρ, is the sliding inner product between the template, h, and the data, s, normalized by the frequency content of the noise, S_n integrated over frequency or time, or $< s|h >$. For example:

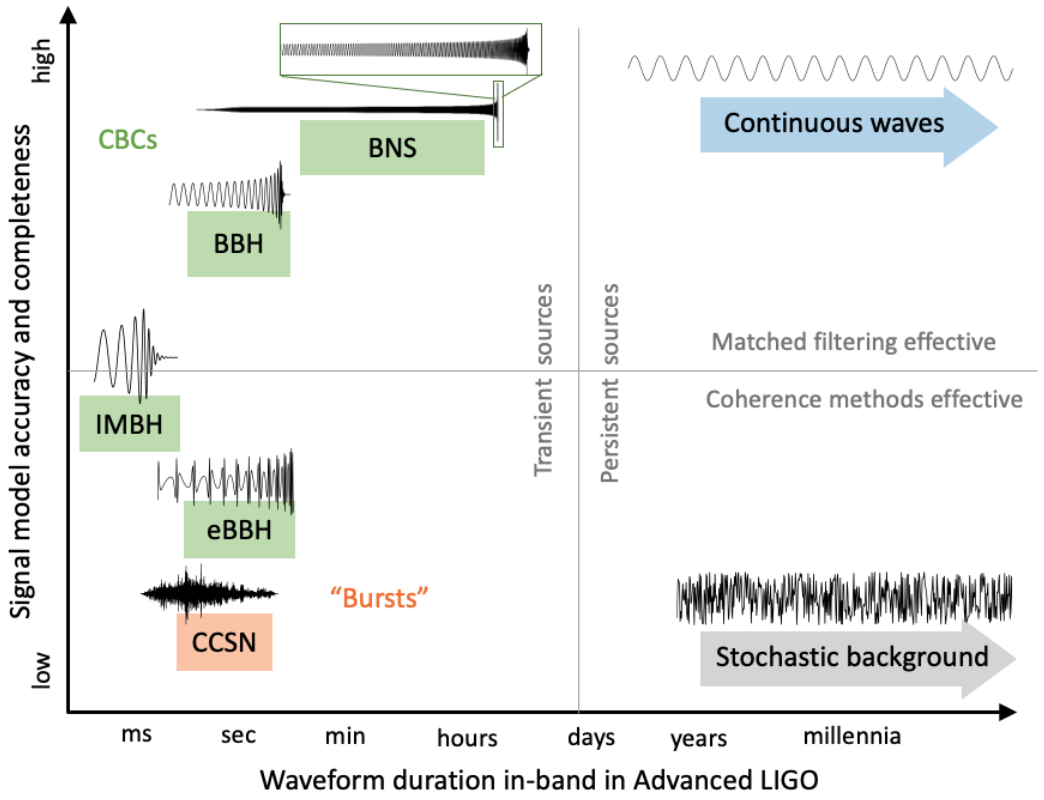

Figure 3. Examples of target GW sources for Advanced LIGO shown by how well current waveform models capture the signal and how much time the signal would spend in the detectors' sensitive frequency range, or "in band". This is useful to understand which data analysis may be most effective for an expected GW source. As we will discuss in Section 4.3, the better modeled the signal, including binary neutron star (BNS), binary black hole (BBH) systems, the more effective we'd expect matched filtering to be. The less well-modeled the signal, including eccentric binary black hole (eBBH) systems and core-collapse supernovae (CCSN), the more advantageous we expect a model-agnostic coherence approach to be. Intermediate mass black hole (IMBH) systems are currently on the border between effective approaches.

$$< s|h >= 4Re \int_0^{\inf} \frac{s(f)h^*(f)}{S_n(f)} e^{2\pi i f t} df \tag{6}$$

We can think of this cross-correlation calculation as sliding a stencil of our template across the data of each GW detector. If there is sufficient GW signal power that is well described by our template present in the data, our cross-correlation will yield a high enough ρ that it is unlikely due to a Gaussian noise fluctuation[5]. Usually if ρ exceeds roughly 8, this time will be flagged as a candidate GW event trigger. CBC searches calculate this matched filter SNR as a function of time for hundreds of thousands of potential Advanced LIGO CBC signals ranging from 1 $M_\odot$ to over 100 $M_\odot$. A more detailed discussion of this process is featured in the LIGO-Virgo data analysis guide [29], and we will examine the case of non-Gaussian noise in the next subsection.

[5]If we took a time series (data amplitude vs. time), plotted a histogram of amplitude values, and found that it followed a Gaussian distribution, we would call this time series *Gaussian*. LIGO detector noise is Gaussian much of the time.

Now that we have the output of our matched filter search, a set of candidate event triggers for each of our detectors, we can use the powerful noise rejection constraint of multiple detectors to look for only coincident triggers due to true signals which propagated through the detector network. General relativity tells us GWs travel at the speed of light, so a gravitational wave could take up to ∼10 ms to travel between the two LIGO detectors (for a GW incident along a line connecting the two LIGO sites), depending on which direction a GW signal comes from in the sky. Knowing this, we can define a network SNR, ρ_{net} as the quadrature sum of ρ for each detector in our network: $\rho_{net} = \sqrt{\rho_1^2 + \rho_2^2 + ...}$ Now our task is to evaluate the significance of this trigger, or how likely it is that random noise manifestations in our detectors could have produced a trigger with an equivalent ρ_{net}. By comparing a trigger's ρ_{net} to the rate at which noise events produce similar triggers, we can calculate the *false alarm rate*.

The LVK Collaborations also perform searches for unmodeled transient gravitational wave signals, or *bursts*, in Advanced LIGO data. Here instead of assuming a template model for the waveform, we can search for coherent gravitational wave power across our detector network. This burst search method would capture unmodeled signals of sufficient amplitude, as well as CBCs with true waveforms that differ from current models. This method generally uses wavelets [30] to capture signal power, which makes it significantly less sensitive than matched filtering methods for most expected CBC sources. However it is particularly well suited to capture very short duration signals, like high mass black hole binary mergers. These higher mass systems merge at lower orbital frequencies, which means they only rise above the detector noise for a few cycles before coalescence. For example, although the heaviest BBH event in the LIGO-Virgo GWTC-1 catalog of events [31] was registered by multiple matched filtering searches, it had the lowest False Alarm Rate (FAR [6]) in the unmodeled burst search pipeline 'coherent WaveBurst' or cWB [32].

Longer duration searches apply different strategies with similar themes. Searches for continuous wave sources also used a matched filtering approach, with the neutron star spin as a template. Instead of a transient waveform, these searches use a single frequency modulated by Doppler shifts due to the Earth's motion, integrated over the data from multiple observing runs to increase the signal fidelity [33]. Searches for a stochastic gravitational wave signal employ coherence methods, since correlated data from different detectors might be astrophysical, also integrated for as long a duration as possible [34]. In all cases, the measured SNR of persistent GW sources will increase with more integration time (i.e. more observing run time).

Our 'observation runs', periods of time when the instruments are collecting data, last for months at a time to be able to collect both large numbers of transient signals and long stretches of data to be used for continuous wave and stochastic searches. To date, with the current detectors, LIGO has completed three observation runs, O1, O2, and O3, accruing roughly two years of integrated observation. Virgo joined at the end of O2 and for O3. This has allowed researchers to compile catalogs of signals as well as conduct detailed analyses of exceptional events. The LVK Collaborations take breaks of a year or two between observing runs to improve the sensitivity of the instruments. Increasing the sensitivity of the instruments increases our 'reach' (the farthest sources we can resolve clearly given the constant background of detector noise), and because we detect the amplitude of the wave which falls as $1/r$, the volume of space – and the

[6] The False Alarm Rate is the rate at which we'd expect detector noise to produce an equivalent event candidate by chance.

number of sources – grows with the *cube* of our reach. This makes observing breaks to increase the sensitivity very rewarding in terms of event rate!

4.4. Detector sensitivity and data quality

The *sensitivity* of the Advanced LIGO detectors is often characterized by the *power spectral density* (PSD). A power spectrum helps us characterize the frequency content of the data by transforming the data from the time domain into the frequency domain via the Fourier transform, as shown for LIGO-Hanford in Figure 4. We'll learn more about the noise sources that give the LIGO noise curve its characteristic shape in the next section.

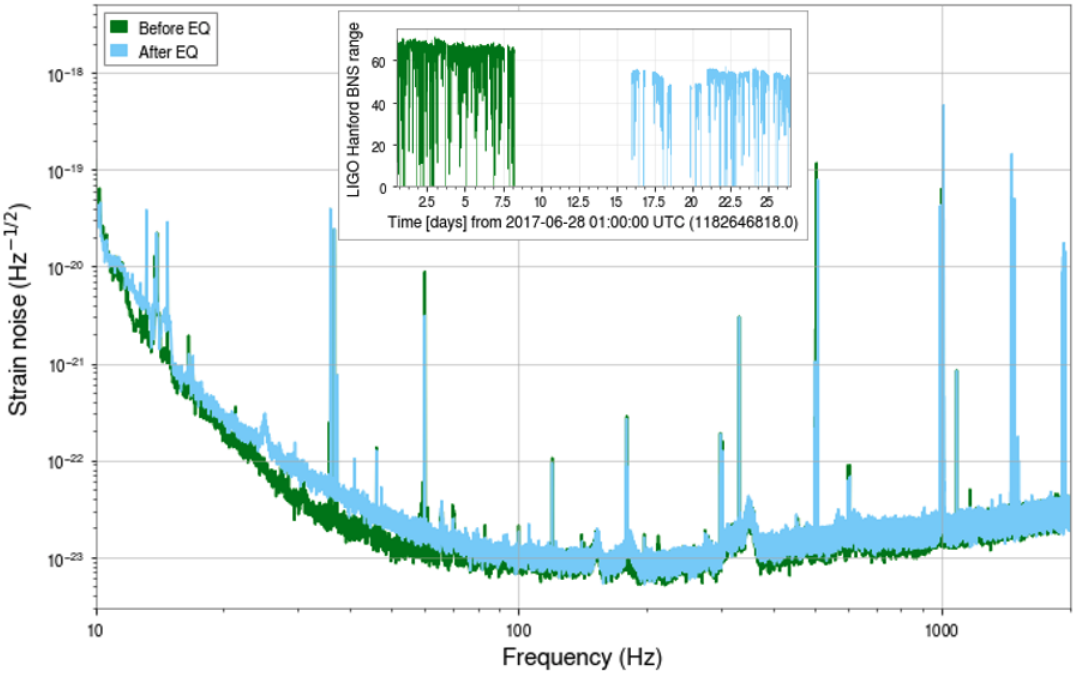

Figure 4. An amplitude spectral density (ASD, which is the square root of the PSD) plot shows the LIGO-Hanford data amplitude vs. frequency over a five-minute period before and after a nearby earthquake in June 2017. The binary neutron star inspiral range for two weeks before and after the earthquake is shown in an inset. An apparently subtle change in the spectrum produces a large effect in the effective detector range! *credit as needed*

We can also conveniently characterize detector sensitivity with a single number; the *range*, a measure of the distance an Advanced LIGO detector would be able to detect a particular reference source[35]. The range depends a great deal on the strength and frequency content of the source. Historically the Advanced LIGO detectors have gauged their sensitivity in terms of the binary neutron star range: the distance at which the detector would register a 1.4-1.4 $M_\odot$ binary neutron star signal with an integrated SNR of 8, averaged over all possible sky positions and source orientations. Figure 4 shows how a relatively subtle change in the frequency content of detector noise can correspond to a significant change in range by highlighting the change in range due to new noise couplings introduced into the LIGO Hanford data after the detector was shaken by a nearby earthquake during the second Advanced LIGO observing run, O2. Those new couplings were tracked down to electrostatic charging of the interferometer

optics when they rubbed against nearby safety stops during the earthquake; this kind of sleuthing is central to bringing the instrument to its best sensitivity.

You may notice the binary neutron star range in the inset of Figure 4, often dips below the median characteristic range, which is governed by relatively stationary detector noise. Some of these fluctuations away from nominal stationary noise are caused by slow (< 1 Hz) shifts in the detector's operating configuration, such as where the laser beam is falling on each optic. The shorter duration, sharp dips in range are due to *glitches*, or bursts of transient noise, in the detector data. Glitches can mask or mimic true transient astrophysical signals, as well as interfere with accurate inference of astrophysical source properties in cases where glitches and true signals overlap. Short duration glitches occur as often as a few times per second in the Advanced LIGO detectors, and glitches as loud as the one shown in the top panel of Figure 5 occur roughly once every hour. Compare this with the expected duration of transient gravitational wave sources in Figure 3! Effectively mitigating transient noise is an active area of ongoing LIGO detector characterization research.

You may also notice many features that look like vertical lines sticking up from the noise curve in Figure 4. These noise artifacts obscure searches for long-duration gravitational wave sources at those frequencies. They look like 'lines' because we're viewing them in the Fourier domain; there is a high amplitude sinusoidal component of the noise at these frequencies. The strongest of these line features, those that are easily visible in an ASD averaged over five minutes of data, are largely understood. The lines at roughly 15 and 35 Hz are injected into the data by the photon calibrator (see Section 6) in order to produce a continually accurate calibration of detector data, which transforms detector sensor and control signals into estimated spacetime strain. The lines at 60 Hz and harmonics are due to the AC power grid in the U.S. (The Virgo detector has similar lines at 50 Hz, the AC power frequency in Europe.) The lines at 500 Hz and harmonics are 'violin' modes, mechanical resonances associated with the fused silica fibers used to suspend the optics that make up the interferometer arms. We will learn more about these detector components in Section 6.

Looking at the top panel of Figure 5, we can see a potential problem with our simple definition of SNR from the last section, ρ, as the inner product (as a measure of similarity) between a template and our detector data. This cross correlation statistic can also produce a high SNR trigger for a loud glitch! We can mitigate this problem by looking in more detail at the match between the template and the data. We will redefine ρ by re-weighting it, usually by multiplying by a weight between 0 and 1, based on a metric that evaluates how well the data matches a given template. One strategy commonly used is the χ^2 method employed by the PyCBC algorithm, illustrated for both a loud glitch and a true signal (GW170814) as a time series in Figure 5. The χ^2 method divides the template into frequency bands of equal power and calculates the relative power in the data in those same bands [36]. If there is a good match between the signal template and the data, the re-weighted SNR, ρ', is largely unaffected, whereas if there is a mismatch, ρ' will decrease [37]. Note that this strategy is not as effective when target signals share similar time frequency morphology with common detector glitches. For example, blip glitches can limit our ability to confidently detect higher mass signals [38].

Results from GW searches to date are discussed below in Section 8. We first look a bit more closely at the detectors themselves.

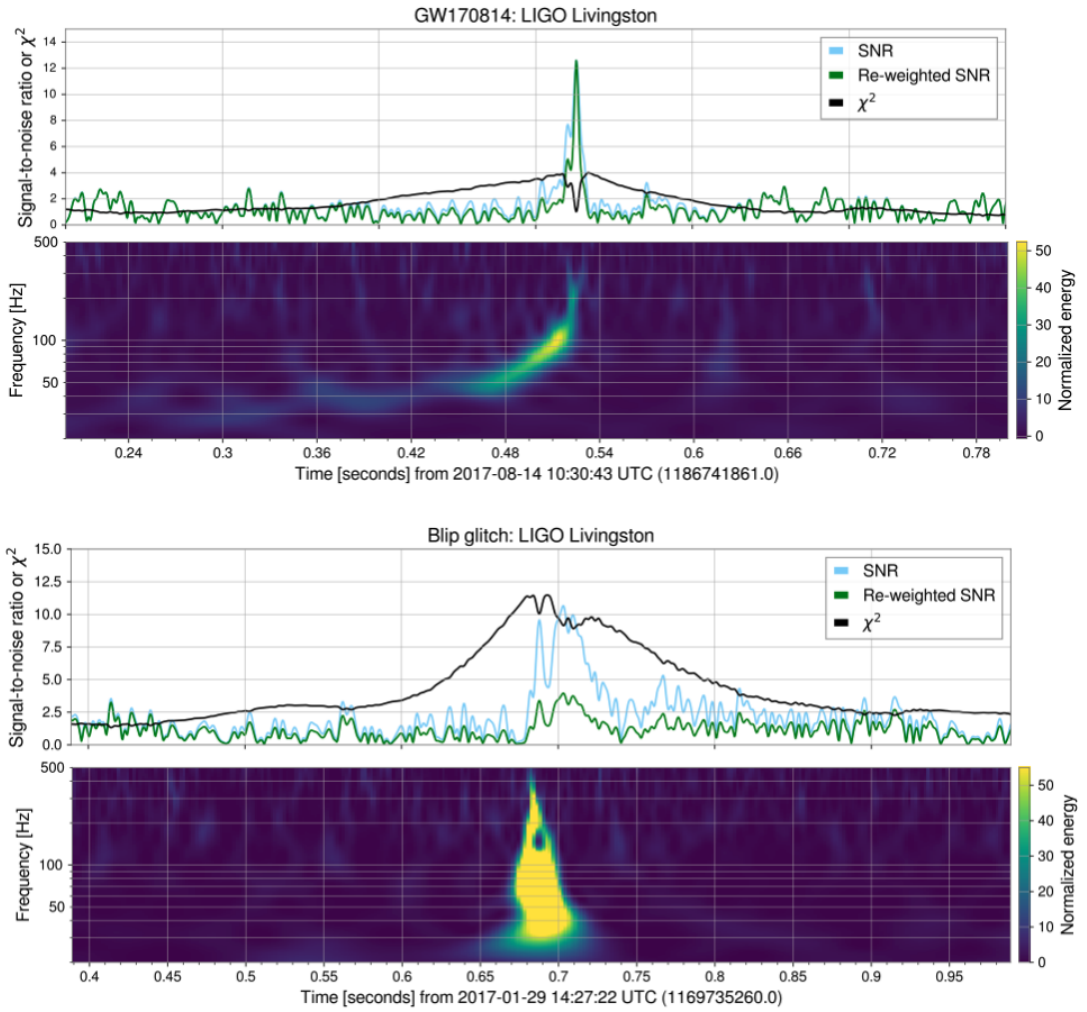

Figure 5. Matched filtering SNR and data visualization for an astrophysical signal (GW170814, above) and a common Advanced LIGO blip glitch (below). For both the true signal and the detector glitch we show the matched filter SNR (light gray trace), the χ^2 time series showing the match between the data and an astrophysical template, and a q-scan which shows the time-frequency evolution of the data. SNR that is re-weighted by χ^2 captures the true signal with equivalent SNR, and rejects the glitch with an time-frequency evolution that does not match the template. *need to request permission*

5. Basic noise sources

With an understanding of the basic mechanisms for gravitational wave detection, we can now look at what limits our detector sensitivity. It is helpful to break down these limits into two categories: the ability to sense the difference in the round-trip light path for the two arms, and the changes in this path due to unwanted physical motion of the mirrors at the ends of the interferometer arms.

5.1. Sensing limitations to sensitivity

As noted in Section 3, the average light intensity on the output 'photodiode' (which converts light intensity into an electrical photocurrent) of the interferometer (see Figure 2) changes as the difference in the arm length changes, and increasing the laser

light power illuminating the interferometer increases the change in intensity for a given strength of gravitational wave. Thus, we would like to work with a powerful laser.

However, there is a fundamental property of light that limits our ability to determine the light intensity exactly, and as a consequence limits our ability to determine the difference in the lengths of the arms, ΔL, exactly. The laser light fluctuates randomly in intensity, and that means our estimation of ΔL also fluctuates; this is a source of noise. Light can be described as a stream of photons – individual particles – and those photons arrive randomly in time. The rate of arrival for a 1 watt laser beam is very high, roughly 10^{25} photons per second. That rate fluctuates; sometimes in one second there are a few more photons, sometimes fewer. This fluctuation is well described by 'Poisson' statistics, which predict a fluctuation from second to second as proportional to the square root of the number of photons in one second. If we had a very weak light beam with only 10 photons per second on average, and we counted photons arriving each second, we would expect to see fluctuations in the number of about $\sqrt{10} \sim 3$, so a series of measurements might show 8, 10, 7, 13, 11, 10, 12,.... photons per second – fractional fluctuations on the order of $\sqrt{10}/10$ ∼30%. Now suppose we had a beam of 100 photons per second. The fluctuations should be of order $\sqrt{100} = 10$. But the *fractional* fluctuations will be of order $\sqrt{100}/100$ ∼10%, so we have improved our precision by increasing the light power P (which is proportional to the average number of photons/sec). Our uncertainty in the actual position of the masses due to this effect scales as $1/\sqrt{P}$, and of course with the 'integration time' over which we look at the signal – a longer integration time counts more photons, and so with smaller uncertainty. We need to be able to estimate the signal amplitude of our GWs with an integration time of say 1/100 second, which increases the rate of photons needed. With our 1 watt beam and 10^{25} photons per second, the fluctuations now are on the order of 3×10^{12}. In operating detectors, we have equivalent light powers of thousands of watts; this enables a sufficiently precise measurement of the light power leaving the interferometer, and thus of the arm lengths. We will see below that the final interferometer is more complicated, but much of this complication serves to ensure that we have as many photons per second – or light power – as needed to resolve the tiny arm length changes that are made by passing gravitational waves. We call this uncertainty in the photon number the 'photon shot noise' and it *decreases* with increasing laser power.

There is a downside to increased laser power, however. Each photon hitting a mirror in the interferometer transfers a bit of momentum to that mirror. The same random arrival rate of photons means that there is a random force on the interferometer mirrors, which causes them to jitter in position and potentially 'mask' the very subtle motions due to gravitational waves. This 'radiation pressure' force noise *increases* with laser power; the motion of the effectively free optics of the interferometer arms scales as $\sqrt{P/(mf^2)}$, with P the power, m the mass and f the observation frequency, due to the inertia of the mass. This leads us to make the mirror as massive as possible – bigger m means smaller motion due to this light momentum effect.

We now have two rather fundamental quantum[7] 'sensing' effects which are complementary; higher power P leads to better resolution of the light power at the output of the interferometer, but also leads to more motion of the interferometer mirrors (growing at lower frequencies as $1/f^2$). This leads to the 'standard quantum limit' – for this configuration, there is an optimum power to use for measurements at a given frequency. It is interesting to note that Einstein was the first to identify the quantum

[7]In this case, when we use the term 'quantum', we mean the quantum of electromagnetism, the photon.

nature of light to explain observed phenomena. These two limitations to sensitivity or noise sources are usually combined into a single 'quantum noise' curve in plots of sensitivity (see Figure 6). Further details at an introductory level on this and the other effects mentioned in this section can be found in [19], and at a more sophisticated level in [39]. Worth noting is that LIGO recently observed this effect in its detectors [40] – one of the examples of fundamental physics research made possible by these beautiful instruments.

5.2. Physical motion limitations to sensitivity

Another fundamental limit to detector sensitivity is thermal noise, and again an effect first explained by Einstein. Thermal noise is observed as small-scale random motion in all objects due to their physical temperature. Technically, temperature is defined as the average random motion. This is most familiar through the observation of Brownian motion – the random walk of particles due to collisions with molecules moving with thermal energy, reflecting the fact that at non-zero temperature, all parts of a macroscopic object have random kinetic energy. Similarly, a mechanical system of a mass on a spring, or mass hung as a pendulum (as are the mirrors of our detectors – see Section 6), also will have thermal excitation, and will exhibit random motion. Remarkably, this is visible even in our 40kg optics. Ising [41] and others showed that the root-mean-square thermal motion (the integral of the noise spectrum) scales as $\sqrt{k_B T/k_s}$, where k_B is Boltzmann's constant, T the temperature (in Kelvin), and k_s the spring constant (or more generally a characteristic of the potential energy stored in the system). In a pendulum, like the ones that support our interferometer arm mirrors, the energy is stored in the earth's gravitational field (when the pendulum swings to the side, it lifts up a bit, storing energy mgh where m is the pendulum mass, g is the Earth's gravitational constant, and h is the increase in height of the pendulum bob above the lowest point). We also want to know how this motion is distributed in frequency, and quite generally, the thermal motion in a resonant system is concentrated at frequencies close to the resonance (this is a consequence of the 'Fluctuation-Dissipation' theorem [42]). In a mass-spring system, that might be due to friction in the spring; for our GW detector mirror pendulum, it is likely due to bending losses in the fused silica fibers that suspend the mirror.

To manage this source of noise – real physical motion of the interferometer mirror due to its thermal energy – we can try to reduce the temperature, but since the motion goes with the square root of the temperature, dramatic reductions are needed to have a significant effect. More subtly, we can also seek materials and construction methods which minimize the mechanical losses. This does not reduce the integrated motion of the object, but concentrates the motion at the frequency of resonance of the system, and reduces the motion above and below the resonance.

This leads to many of the detailed design decisions in the mechanical structure of the detectors. We make pendulums and the mirrors themselves out of very low-mechanical-loss materials, such as highly pure fused silica glass, which if struck (gently!) with a hammer would ring for a million seconds. Even the reflective optical coatings on the mirrors are made of materials which, in addition to making an excellent reflective surface, must minimize the extent to which they 'damp' their internal motions, and this is currently a limit to our sensitivity. Several thermal noise sources are shown in Figure 6. The 'Suspension Thermal' noise is that due to the pendulum suspension of the mirror; 'Substrate Brownian' is noise due to excitation of the mirror itself; and the

'Coating Brownian' is the noise due to the motion of the very thin reflective coating on the mirror – and it is the most important noise source around 100 Hz.

Another important limitation to terrestrial gravitational-wave detectors is motion of the ground due both to human activity but also wind, water waves, and Earth's seismic activity [43]. It varies by locale (e.g., distance to the nearest ocean, the local and regional composition of the Earth, proximity to cities and highways, etc.), but generally is large at low frequencies and falls as $\sim 1/f^2$, where f is the frequency. Systems to filter or suppress this motion will be discussed in the next section, but here we note that very efficient filtering has pushed this as a direct source of unwanted motion of the mirrors to be negligible above roughly 10 Hz (for Advanced LIGO).

However, an effect of seismic motion which cannot be filtered is that due to Newtonian noise. Seismic motion propagates as waves, in for example, compression of earth propagating at the speed of 'sound' in the Earth's surface [43]. Thinking in terms of Newtonian gravity, the mirror, suspended as a pendulum, is attracted to the distribution of mass around it, but the distribution dynamically changes due to e.g., seismic waves; the mass is pulled toward the more compressed, denser earth, and as that compression wave passes, the mirror to some extent follows it. (Someone walking by also gravitationally 'attracts' the mass, and could also be a problematic noise source!) This random force on the mirrors dominates at around 7 Hz and lower frequencies, hiding any GW signals, and appears to be a lower frequency limit for terrestrial gravitational-wave detectors on the surface of the Earth. One can move that wall down to say 3.5 Hz by putting the detector far underground, where the seismic noise is less. Happily there is a lot of exciting astrophysics to be done at higher frequencies, but access to lower frequencies will require mirrors far from the Earth's noisy environment. There is just such a project in preparation, the Laser Interferometer Space Antenna or LISA, that we will mention briefly below.

This set of basic limitations to the sensitivity is shown schematically in Figure 6. We see that the best sensitivity is around 100 Hz, where the quadrature sum of these nominally independent noise sources is at a minimum.

6. Description of Advanced LIGO as an example

A great deal of refinement and additional complexity is needed to take the concept of a simple Michelson interferometer and convert it into a working detector of sufficient sensitivity, reliability, and stability to read out gravitational waves. Here we will focus on the requirements and the conceptual design; there are great resources for plunging more deeply into the process [12,39].

Figure 7 shows some of the complexity of a working detector. Let's look in more detail at other elements of this layout.

Laser: The laser and input optics subsystems are required to deliver a beam of order 100 W power to keep the statistical photon noise low. The laser also needs to propagate the full 4km length of the arms without spreading out to be larger than the end interferometer arm mirrors; to do this a collection of curved mirrors (in the 'Input Optics') expands the laser beam – like using an optical telescope in reverse – and focuses the beam around half-way down the arms. The detectors employ a neodymium ytterbium-aluminum garnet (Nd:YAG) laser, with a wavelength of 1.06 μm. Beam sizes are held close to the minimum possible to help in mirror fabrication, leading to a Gaussian beam (TEM_{00}) of the order of 10 cm diameter for path lengths of 4 km [45]. The technical intensity fluctuations – not those due to the random arrival

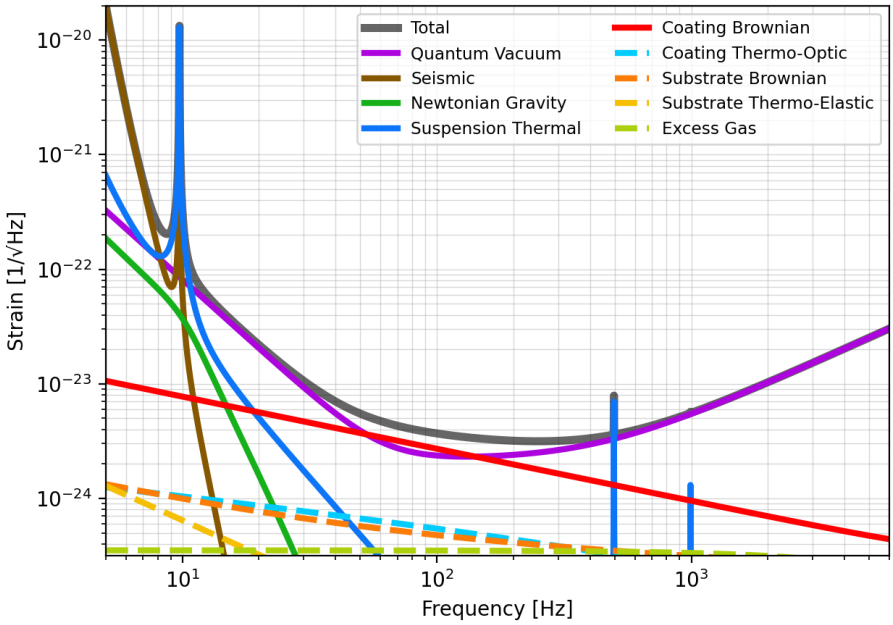

Figure 6. Basic Advanced LIGO noise sources as a function of frequency. The levels correspond to the detector design parameters. The 'Quantum Vacuum' trace represents the contribution from shot noise at high frequency and radiation pressure at low frequency. The 'Coating Brownian' is the dominant thermal noise term. At low frequencies, the 'Newtonian', 'Suspension Thermal', and 'Seismic' terms limit the lowest frequencies where GWs could be seen to about 10 Hz. The 'Excess Gas' noise is due to the residual molecules of gas in the 4km long path. *pygwinc Gravitational Wave Interferometer Noise Calculator [44]*

rate of photons, which is always there, but rather dimming and brightening of the beam due to technical noise in the laser – must be held to a very tight tolerance, since those changes in intensity also change the light pressure on the interferometer arm mirrors, shaking them and masking the GW signal. The frequency (or equivalently the wavelength) of the laser also needs to be very carefully matched to the natural resonant frequencies supported by the Michelson 'arm cavities' as explained in the next section.

Arm Cavities: We add an input mirror in each arm of the Michelson, close to the beamsplitter (See Figure 7). This mirror allows a few percent of the light through, in contrast to the mirror at the end which reflects 0.9999 or so of the light back. The two interferometer arm mirrors form a 'Fabry-Perot cavity' [45]; this optical system is resonant for light of the right wavelength (such that an even number of half-wavelengths fit exactly in the length of the cavity). The effect is analogous to the effect of singing the note that is resonant in a bottle – one can hear and feel how the sound pressure is amplified by the resonance. In the Fabry-Perot cavity, some light leaks in through the mirror closer to the beamsplitter, and if the light is at just the right frequency, it excites the resonance of the cavity and the power of the light inside this cavity will be of the order of 100 times greater than the original laser light. This larger light power ultimately improves the sensitivity of the detector. We use this principle of light resonance in cavities in many places in the complete interferometer system.

Mirrors: The interferometer arm mirrors at the ends of the Fabry-Perot cavities play a central role in the detector. They must reflect the laser light with minimal scatter and absorption, resist the photon momentum via their mass, while minimizing their contribution to thermal noise through low internal friction. We form our mirrors

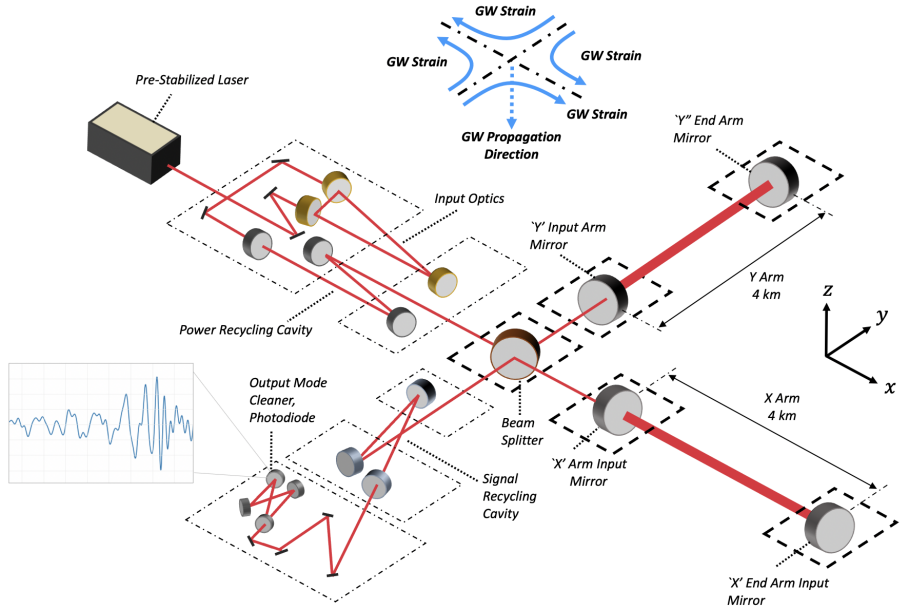

Figure 7. Realistic interferometer schematic layout, showing the main optical components (in grey) and the light path (in red). A few elements of the simple Michelson are evident: the laser to the upper left, the beamsplitter in the middle, and the interferometer arm mirrors at the end of the optical paths on the right side. To set the scale in LIGO, the distance from the beamsplitter to the mirrors at the ends of the interferometer arms is 4km. *F. Matichard/LIGO Laboratory*

out of beautiful cylinders of fused silica – a highly refined form of glass. For Advanced LIGO, these mirrors are 34 cm diameter, 20 cm thick, and weigh 40 kg (around 100 pounds). To minimize scatter of light, the mirror is 'figured' to a precision of 1/10000 of the wavelength of our laser light (so ∼0.1nm). We often refer to these interferometer arm mirrors as 'test masses' in reference to the language of tests of general relativity. An ideal test mass responds to the gravity of other bodies but, in comparison, has negligible gravity of its own. It neither self-gravitates nor distorts the gravitational field of any other body. For our signal sources, the 40 kg mirror fulfills these requirements admirably.

Light Recycling: The resonance technique is also used to increase the intensity of light hitting the beamsplitter, via the power recycling mirror (see Figure 7). This mirror again is partially transparent, and if the distance from the recycling mirror to the average optical cavity lengths in the interferometer are an integer multiple of the wavelength of the laser light, there will be resonance giving another ∼30 times increase in the light intensity in the interferometer, further improving the sensitivity.

There is also a semi-transparent 'signal recycling' mirror at the output of the interferometer. This can be thought of as forming an additional resonant cavity but now for the gravitational-wave signals impressed upon the laser light, and this can boost the strength of the signal in a desired frequency range. This technique also has a very interesting effect of coupling the light intensity changes to interferometer cavity lengths. We saw above in the discussion of basic noise mechanisms that light bouncing off a mirror exerts a force over the area of the mirror – a pressure – on the mirror. Greater light intensity makes a larger force, smaller intensity a smaller force. The signal recycling mirror sends some light back to the interferometer, so that fluctuations in intensity move the mirrors, which in turn changes the resonance condition a bit

away or towards perfect resonance, which changes the intensity. This linking of the two effects due to light resonance and light pressure leads to changes in the response to gravitational waves, and can be used to play with the so-called 'standard quantum limit' discussed above, doing better at some frequencies at the expense of others [46]. Another technique in use, light 'squeezing', plays with the statistics of the light and quantum uncertainty; we say a bit more in Section 9.

Photon Calibrator: A fun application of this light pressure is found in the aLIGO calibration system. We need to know quite accurately the sensitivity of our detector, as it is crucial to estimating the astrophysical properties of a signal. We measure the sensitivity by pointing an auxiliary laser of about 1 Watt power at one of the interferometer arm mirrors and modulating its intensity sinusoidally. This pressure causes the mirror to move sinusoidally, and knowing well the absolute light power and the mass of the mirror we can calculate the physical motion of the mirror, and observe the resulting signal at the output of the detector. In this way, the calibration can be established to about one percent in precision.

Seismic Isolation and Suspension: Any unwanted motion of the interferometer arm mirrors can mask the effect of gravitational waves. Thus we must have systems to reduce seismic noise, and to control the position and pointing of the mirrors. We suspend the mirrors as a pendulum with four glass fibers of 1/2 mm diameter and about 60cm long; we use four so that we can adjust the angle (in tip and rotation) of the optic from above like a marionette.

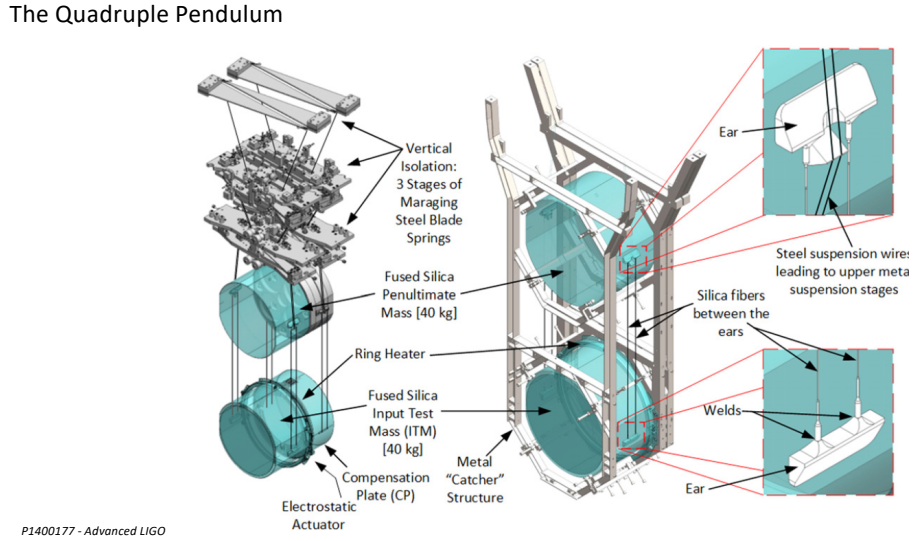

Figure 8. Arm optic suspension. Left panel: The four levels of pendulum, with the bottom two of fused silica glass. There are two 'chains': one with the interferometer optic and the bottom, and one behind which provides a quiet place from which we can exert electrostatic forces on that interferometer optic. The pairs of fibers allow control over the tipping motion (pitch) and the rotation (yaw) of the optic. Right: The protective 'cage' is shown around the components, and some of the details of the fused silica glass suspension are shown. *from Reference [47]; need to ask CQG for permission*

We use a pendulum suspension for its ability to protect the interferometer optic from seismic motion. We call the ratio of horizontal pendulum bob motion for a given motion of the top of the pendulum string the *transfer function*. For a simple pendulum the motion of the pendulum bob falls as f_0/f^2, where f_0 is the pendulum resonance frequency and f is the measurement frequency. This relation comes directly from the inertia of the mass, and the fact that the force required to move a mass is $F = ma$

where m is the mass of the optic and a is the acceleration. Let's look at the properties of a pendulum; consider making one out of string and a weight and carrying out the following experiment. If you move the top of the pendulum back and forth slowly compared to the natural resonance frequency of the pendulum, the pendulum bob (for LIGO, a 40 kg optic) will follow the top motion. If you move the top back and forth at the frequency of resonance (which for our pendulums is ∼0.65 Hz, or about 1.5 seconds for a full cycle), the motion of the optic could become very large; we call this factor of amplification Q, and for our suspensions that number can be millions. But now if you move the suspension point back and forth rapidly compared to the resonance, the optic will not move much, and the higher in frequency the motion at the top, the smaller the motion of the optic will be. We see that the transfer function value is 1 (motion at the bottom is equal to the motion at the top) for frequencies much lower than the resonance; the motion of the optic at resonance at the resonant frequency is Q times the motion at the top; and above this resonance the motion is progressively smaller as the excitation of the suspension point moves at higher frequencies. For a pendulum with a 1 Hz resonance, the motion of the pendulum 'bob' (or mirror in our case) at 10 Hz will be a factor of $f^2 = 10^2 = 100$ times smaller than the motion at the top; we can see that this is an excellent way to attenuate seismic noise. Putting pendulums in series multiplies this effect (two 1 Hz resonance pendulums gives $100 * 100 = 10000 = 10^4$ times attenuation at 10 Hz, approximately).

Advanced LIGO uses four pendulums in series to deliver much of the required seismic isolation; see Figure 8 for a drawing of the system. This 'quadruple suspension' is supported from a platform (a mounting surface) that uses servo controls to further reduce motion. A servo control system (or 'servo') uses a sensor, a feedback amplifier, and an actuator. One familiar example is an oven, which has a temperature sensor, a heater element, and a controller to convert the sensor signal to power to the heater. For Advanced LIGO, the servo controls use a motion sensor (basically a little pendulum with a detector of distance between the pendulum and its support structure), an electrical amplifier, and an electric motor based on the same principle as a music loudspeaker: electricity in a coil makes a magnetic field, which interacts with a magnetic field from permanent magnets [48]. A well-designed servo control system can control the platform to be as motionless as the sensor. We use low-noise seismology sensors which sense motion in all six 'degrees of freedom': translation along x, y, and z, and rotations around each of those axes, and magnetic motors also placed to control all those motions. The result of this combined pendulum and servo isolation system, shown in Figure 6, is that seismic noise can be held below other noise sources for all frequencies higher than about 10 Hz.

Thermal Noise Engineering: The basic concept of thermal noise and our approach to it – seeking mechanical systems with very low internal friction – was mentioned above. It is worth discussing how the instrument designers achieve the goals. Thermal noise plays a dominant role in the most sensitive elements of the detector: the interferometer arm mirrors and their suspensions.

- Suspension fibers: The four fused-silica suspension fibers are drawn from rods that are heated by infrared lasers; they have a special tapered shape that minimizes the thermal noise motion generated in the fibers. These fibers do have resonances like those of a musical instrument string (we call them 'violin modes'), and just like everything in the detector have thermal energy which excites these modes. They can be seen as narrow spectral features in Figure 4 because some of the fiber motion is carried to the optic below. These fibers assure that the

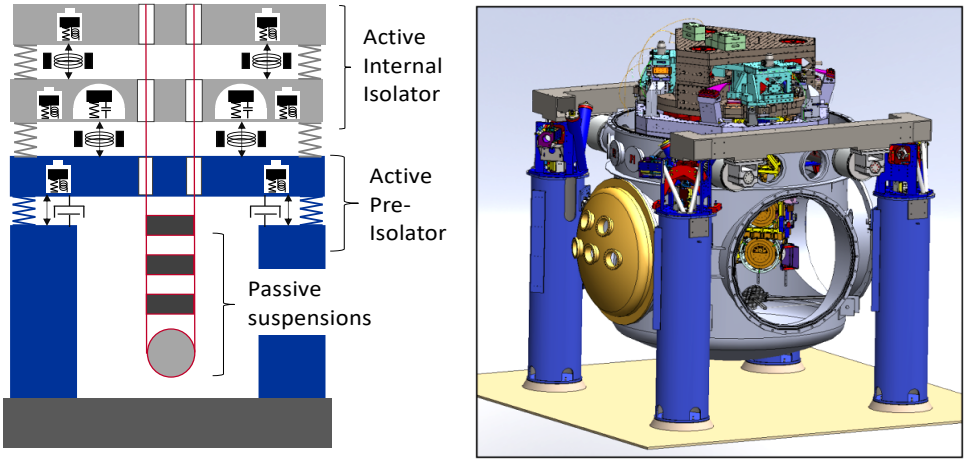

Figure 9. Left: In this schematic diagram, the quadruple ('Passive') pendulum is shown hanging from a multi-stage servo-controlled platform. Right: In this computer rendering, the isolation system is primarily housed inside the LIGO vacuum system, shown in cutaway; external supports are in blue, and include one additional isolation layer. *F. Matichard/LIGO Laboratory*

broadband *pendulum* thermal noise is small enough to not interfere above about 10 Hz with GW detection – we can in general ignore the narrow resonances.

- Optics: The optics, as said earlier, take the form of a 40 kg cylinder of ultra-pure fused silica glass. This material has remarkably small mechanical internal friction, so that the thermal energy is almost entirely gathered into the mechanical resonances of the cylinder. We choose the form of the cylinder – 35 cm diameter, and 20 cm thick – to make the resonance frequencies as high as possible to avoid the detector sensitive band; the lowest is 6.8 kHz. All sides of the cylinder are polished, both to provide a good optical surface on the faces, but also to reduce mechanical friction.
- Assembly technology: Again to reduce friction, the interferometer arm optic, the suspension fibers, and the final states of the mirror suspension are joined by polishing the pieces to be flat to a fraction of an optical wavelength (better than 10^{-7} m) and then placed together with a solution of silica (glass) powder in liquid. Under pressure, the pieces of glass join together as a single 'monolithic' object, free of unwanted resonances and very low in friction, and therefore thermal noise.
- Optical reflective coating: The reflective coating is made up of alternating layers of materials of high and low refractive index; this is a well established approach to make optical coatings of low absorption, high reflectivity, and very little unwanted scatter of light. The total coating thickness is only of the order of 0.1 mm, but it turns out these materials have much greater internal friction than the glass mirror itself, and so this thin coating dominates the thermal noise in the band from about 10 to 100 Hz. Note that the mechanism for mechanical internal friction is basically different than the mechanism for optical absorption – both need to be independently optimized [49].

The thermal noise engineering of gravitational-wave detectors remains one of the most challenging aspects. In particular it is the focus of research at this time to find coating materials and processes which can reduce the thermal noise in the 10-100 Hz fre-

quency range. Ultimately, future generation ground-based detectors will likely pursue techniques for cooling the optics and suspensions of gravitational wave detectors, as a way of reducing the thermal noise.

Control of the complete system: We have mentioned the need for the various optical cavities to be in resonance with the laser light. In practice this means that the lengths of all of the cavities need to be held to within a small fraction of a light wavelength – on the order of 1/100 of one micron, or wavelength of our laser light – to maintain resonance. It is also necessary to maintain the *angular alignment* in pitch and yaw (See Figure 8) of the mirrors with the laser beam. One can see roughly how much precision is needed by noting that the light from the 4 km-distant interferometer end arm mirror needs to return to be well centered on the near 4 km mirror. Say we require the beam to be returned within 1 mm of the center over 4 km; then we need angular control of 4×10^{-6} radians, or roughly a tenth of a degree. With roughly 15 optics to control simultaneously, we require around 45 servo control systems, all of which need to work together to high precision.

Physical Environmental Monitor: The Advanced LIGO detectors have an array of sensors that attempts to cover all of the environmental influences on the instruments that could arrive at multiple detectors roughly simultaneously, and many that could lead to excess noise in the instrument or mimic a GW signal. There are microphones, accelerometers, seismometers, cosmic-ray monitors, weather stations, short-wave radios, and cameras distributed around the observatories. We choose sensors which *should* be more sensitive to environmental disturbances (by design) than the interferometer is (by accident). In this way, we can always check if a signal is due to say a lightning strike or other disturbance instead of a gravitational wave.

The Vacuum System and Buildings: The last 'subsystem', but in fact the most expensive one, that must be discussed is the physical infrastructure. The laser light needs to travel 4 km from the beam splitter and 'near' input mirrors of the Fabry-Perot cavities to the end interferometer arm mirrors. It needs to travel in a very good vacuum, to avoid the effects of the atmosphere on the beam. There are some evident problems with the light traveling freely in the air, such as the focusing and de-focusing effects of heat gradients (like the shimmering of the image over a highway on a hot day). But even with what is called an 'ultra-high vacuum', there are still remaining molecules of residual air which cross the beam. Those molecules have an index of refraction (due to their polarizability), and make a very small change in the optical path length when they traverse the beam at random times (another Poisson process). We need to provide a good enough vacuum that this noise does not mask the signal due to the passing GW, and this leads to requirements for the quality of the vacuum (hydrogen dominates, and must be less than roughly 0.4 micropascals, $\sim 10^{-11}$ atmospheres), as well as the material and treatment of the 'beam tube'. We also require that the beam tube be much larger than the beam to avoid light scattering from that seismically noisy surface (we choose a 1.2m diameter tube for a $\sim$10cm light beam), and place baffles along the 4 km length to absorb stray light. The vacuum system is a very significant part of the cost of building any GW observatory on the Earth[8].

From the civil construction perspective, we note first that laser light takes a straight path, and the surface of the Earth is curved; over 4 km, one must do some earth moving to ensure that the vacuum pipe can be laid truly straight. A concrete bed and cover is needed to protect the vacuum system from weather and other damage. We also have

[8]And putting it in the vacuum of space is no less expensive!

sizable buildings at the vertex (where the 4 km arms meet) and ends of the vacuum pipes, to accommodate large vacuum tanks for the seismic isolation systems and of course labs and offices for staff members and visitors at the observatories. The two LIGO observatories are almost identical, so altogether we have 16 km of pipe, bed, cover, and a number of buildings to maintain. An aerial view of the LIGO Livingston Observatory in Louisiana, USA, is shown in Figure 10.

Figure 10. Aerial view of the LIGO Livingston Observatory. The protective covers over the vacuum tubes indicate the light path from the corner station (with laser and beamsplitter) to the end interferometer arm mirrors 4km distant. *Reports on Progress in Physics, v.72 (2009)*

The observatories are placed some distance from cities to keep the seismic environment as quiet as possible. Additional constraints for good sites include a level surface to avoid excessive earth moving; relatively low Earth seismicity; compatibility with nearby activities; and a means to acquire the land without excessive cost. Multiple sites, separated by thousands of km, are necessary to enable the localization of signals by looking at timing and other characteristics of the signals (and as a check that signals are truly of astrophysical origin).The two LIGO sites are separated by 3000 km (around 2000 miles; about 10 msec of travel time for light or gravitational waves).

An absolutely critical part of a working detector is the scientific and technical staff. Each LIGO observatory has roughly 40 persons working at the site. There are physicists at all levels – senior, early career, postdocs, and students – who all play key roles in making the detector work well. There are mechanical, vacuum, electronics, and optical engineers, and technical specialists who help install and test each system, and then ensure its operation. Outreach and education specialists help communicate our science to visitors of all ages and interests. Service staff keep the sites running smoothly. Visiting scientists and engineers from the LIGO Laboratory and the LIGO Scientific, Virgo, and KAGRA collaborations round out the roster of almost 2000 people contributing to the observation of gravitational waves with Advanced LIGO.

7. Average noise performance

In the last two sections we learned about the basic noise sources predicted to fundamentally limit Advanced LIGO and the complex array of interrelated subsystems that all can potentially introduce *technical* noise, or noise that could potentially be improved through tuning and commissioning of the detectors and currently dominates over fundamental noise at some frequencies. We can measure our understanding of the noise sources we are aware of and how they add together to govern the average range of the detector, as we saw in Figure 4. A *noise budget* [50] shows a curve of the frequency content of each known noise source, the sum of known noise, and the measured strain noise, as shown for the LIGO Hanford detector during O2 in Figure 11. Notably, we see a gap between the measured strain noise, which is a PSD of the detector data, and the sum of all known noise sources. This is an indication that we did not fully understand the noise that obscures our strain measurements below 100 Hz at the time.

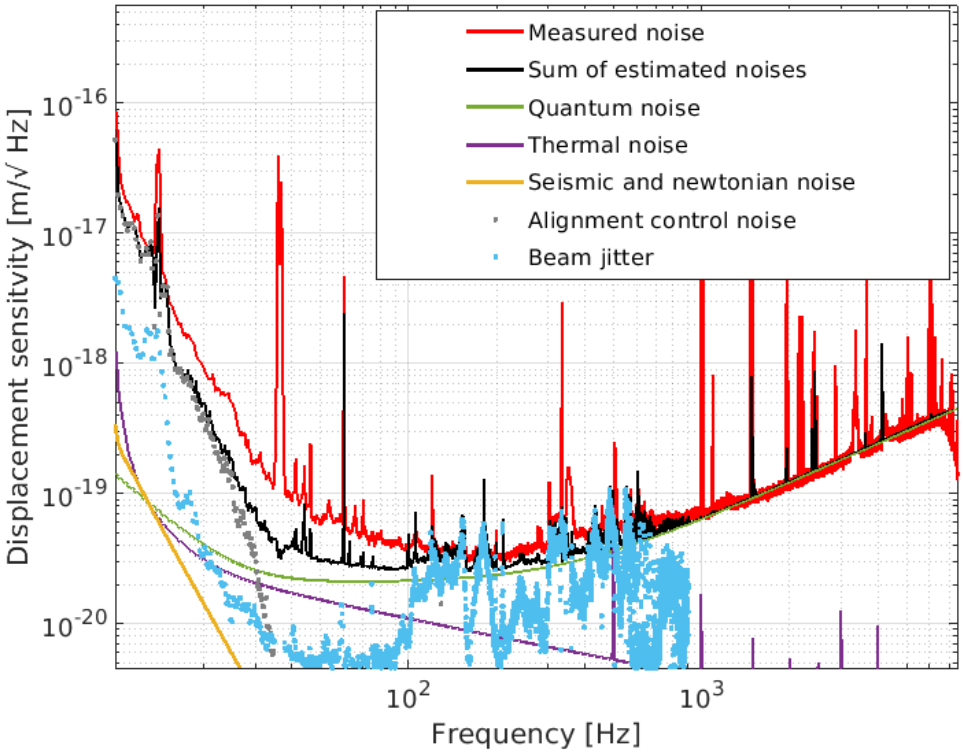

Figure 11. An example of an Advanced LIGO noise budget, from LIGO Hanford during the O2 observing run. The red curve shows the measured noise (a Fourier transform of the detector data without a GW signal present) and the black curve shows the total sum of all known noise sources. The difference at low frequencies is thought to be related to optical cavity angular control noise. Beam jitter noise, in light blue, was introduced through vibrations in the table supporting the input laser (brought about by cooling water shaking the table) and dominated the detector noise at some of the most sensitive frequencies. From LHO alog 35838.

A noise budget is useful to diagnose the stationary and quasi-stationary noise sources most limiting to the detector's sensitivity. Here we see curves for the basic sources of noise: quantum noise dominates above a few hundred Hz, whereas thermal and seismic noise are not yet limiting. A notable example here is *beam jitter* noise, where mechanical vibration of the input laser table was shaking the laser light before it

entered the interferometer during O2. In this case, we had a physical environment monitor, an accelerometer, that witnessed this motion. If we measure the phase and amplitude relationship, or *transfer function* between the time series of the noise witness and our strain data, we can use a simple linear filter [51] to subtract the witness' noise contribution from the data. Subtracting the beam jitter noise with this data post-processing increased the distance to which a BNS could be detected by the LIGO Hanford detector by as much as 50% toward the end of O2 [52]. This is also an effective method for reducing the impact of the 60 Hz AC power lines, which are witnessed by voltage monitors. However, power spectral methods (including noise budgets) are not effective for understanding short duration noise. We need to rely on the methods described in Section 4.3 to mitigate the effect of glitches. Support from LIGO Scientific Collaboration scientists based off-site is helpful in characterizing these noise sources and processing the data to mitigate them wherever possible.

8. Results to date

The Advanced LIGO interferometers detected the first gravitational wave signal from a black hole merger on September 14, 2015. In just five years, the field of gravitational wave astronomy has grown dramatically. The Advanced Virgo detector, which joined the network in the summer of 2017, allowed the LIGO-Virgo network to detect events with the potential for vastly improved sky localization, which was critical for the discovery of the kilonova [53] produced by the binary neutron star merger GW170817 [54]. A third detector also allowed novel tests of general relativity and increased the uptime of the global detector network. Further benefits will accrue as the KAGRA detector improves in sensitivity and LIGO India comes online.

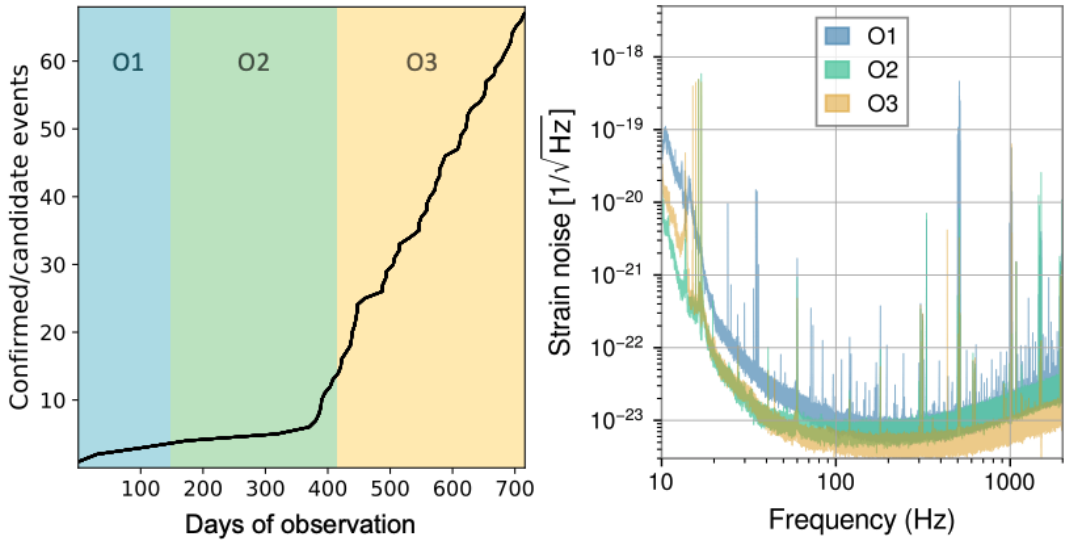

Figure 12. On the left, the cumulative number of confirmed detections in O1 and O2 and event candidates in O3 over time, as they were registered in the data. On the right, strain noise content vs. frequency for the LIGO-Livingston detectors during O1, O2, and O3. Note how a small change in sensitivity, which governs detector range, translates to a large change (distance^3) in event rate.

LIGO and Virgo release gravitational-wave strain data publicly after a proprietary period used to calibrate, clean, and initially analyze the data, currently 18 months.

Using data released on the Gravitational Wave Open Science Center (gwosc.org)[9], research teams outside of the LIGO-Virgo collaboration have independently confirmed these findings and reported additional detections [55,56].

In the third observing run (from 1 April 2019 to 27 Mar 2020, ending a month early due to COVID-19), the LVK Collaborations initiated a program of Public Alerts for candidate events. Each candidate with an estimated False Alarm Rate (FAR) of less than one per month was automatically publicly reported, including information about whether the source was likely to produce a kilonova (an electromagnetically observable remnant) and a map indicating where in the sky it likely originated. This followed a program of agreements with a set of observers for O1 and O2 which was very successful.

During O3, the Collaborations released 56 candidates and have reported 39 events from the first half of O3 [57] as confirmed events. Following deeper analysis, not all remaining reported candidates will be confirmed as significant events in the LVK's upcoming catalog of detections from the second half of the third observing run, but new previously unreported events may be successfully identified after data post-processing, thorough data quality studies and mitigation, and improved calibration. We might assume the total number of confirmed LIGO-Virgo detections after the third observing run will be roughly 70, an increase of nearly a factor of 7 in known gravitational wave events relative to the first two observing runs, with roughly as much total observing time added, as seen in Figure 12.

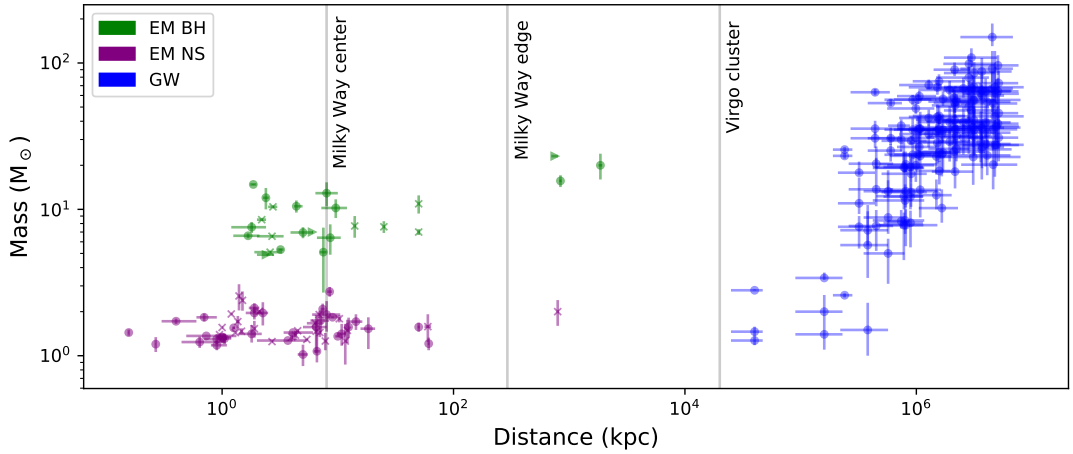

Figure 13. Compact object masses and distances measured with different messengers: electromagnetic radiation and GWs. In purple are neutron star masses estimated via electromagnetically. In green are black hole masses estimated using X-ray emission from a stellar mass black hole and a companion star to calcuate their orbital period, taken from a table compiled by Wiktorowicz and Belcynski. Distances to most X-ray binary sources shown were taken from Jonker and Nelemans's compilation [58] and references therein. Any quantities without a reported error in either mass or distance are marked with an x. Lower limits on mass are indicated with a right-facing arrow. Compact objects with mass and distance estimated with GWs are plotted in blue. A few interesting distances from Earth, the galactic center, the edge of the Milky Way halo, and the Virgo cluster are shown with gray lines.

Since 2015, the Collaborations have reported discoveries with gravitational waves that have revealed an energetic, dynamic Universe beyond what we are able to see with other messengers, including EM radiation or neutrinos. Figure 13 shows the mass and distance of stellar remnants measured with light and with gravitational

[9]You can also find LIGO-Virgo software tutorials, open data web courses, and learning paths on the GWOSC.

waves. Clearly, gravitational waves are probing new regimes of mass, and are able to estimate distance much further into deep space than is currently possible with either radio (used to estimate neutron star mass) or X-ray emission. This new population of black hole mergers, observable only with GWs, may yield clues to their origins.

GW150914: the first discovery of GWs with Advanced LIGO. Just before the expected start of Advanced LIGO's first observing run, the detectors registered the very first direct observation of gravitational waves. With just this initial discovery, physics and astrophysics made major strides forward: the signal of GW amplitude as a function of time matched general relativity predictions; the coalescence was only compatible with effectively point masses, confirming the existence of black holes; and the masses of the black holes that merged (29 and 36 $M_\odot$) exceeded all black hole masses previously measured with X-ray observations [1] revealing an unexpected population.

GW170817: the first multi-messenger discovery. The first observation of gravitational waves from a binary neutron star merger was registered by three GW detectors, Advanced LIGO and Advanced Virgo, yielding a much more precise sky localization in position and distance, which enabled the detection of the resulting kilonova [54]. The detection of GWs, gamma rays, and other EM observations of the kilonova over time from this one event have significantly evolved our understanding of energetic gamma ray bursts and the production of heavy elements [59], the expansion of the Universe [60], the structure of neutron stars' extremely dense matter [61], and allowed us to perform new tests of general relativity [62] – for example, light and GWs propagate at the same speed to within one part in about 10^{15}. During Advanced LIGO's third observing run, a second detection of GWs from a binary neutron star merger, GW190425, revealed evidence for a new extragalactic population of heavy neutron star binaries [63].

GW190814: discovery of a heavy neutron star or a light black hole. This merger was composed of a $\sim$23 $M_\odot$ black hole and a $\sim$2.6 $M_\odot$ compact object [64]. The less massive compact object was the first to be confidently observed within an observational "mass gap" between neutron stars (ranging up to roughly 2.1 $M_\odot$) and black holes, adding to what we have learned about compact object masses through electromagnetic emissions [10]. GW190814 also has the largest difference between the masses of the component objects (the *mass ratio*) of any merger to date, which allowed us to resolve the signature of higher order mode contributions in addition to the quadrupole moment, similar to GW190412 [65].

GW190521: Discovery of an intermediate mass black hole. Gravitational waves provided the first definitive observation of an intermediate mass black hole (a black hole with a mass between 100 and 100,000 $M_\odot$) with the discovery of a binary black hole merger yielding a final black hole with a mass of $\sim$142 $M_\odot$[11]; well above black holes produced by stellar collapse (up to $\sim$100 $M_\odot$) and far less than supermassive black holes at the center of galaxies, like our own Milky Way [66]. The larger black hole had an estimated mass of $\sim$85 $M_\odot$, and over 99% probability of being in a different, predicted black hole "mass gap" due to pair instability supernovae, which placed it in conflict with current theories of stellar evolution [67].

Gravitational waves will continue to reveal new populations of astronomical objects that were previously hidden to us. With GW measurements of the mass, spin, and distance of compact objects, it will be possible to start to distinguish between various

[10] You can find nice visualization of compact object masses estimated using EM radiation compiled by Wiktorowicz and Belcynski here: https://stellarcollapse.org/.

[11] GW190521 released $\sim$8 $M_\odot$ of energy in the final moments of coalescence, outshining all the stars and galaxies in the Universe for a brief moment.

theorized binary formation mechanisms. For example, systems with high mass and high spin may be formed by a hierarchical merger of preexisting black holes in a dense stellar environment, where one or more of the component black holes is the product of a previous merger [68]. GWs may also have already revealed the first hints of the role of intermediate-mass black holes in formation of supermassive black holes at the center of most galaxies [69].

We can use GWs to directly estimate the distance to sources based on the measured strain amplitude. Combined with a redshift measured using EM radiation, we can use GWs to measure the Hubble constant [70], which may help resolve the current tension in measurements based on optical and cosmic microwave background observations [60]. GWs will also give us new insight into the structure of the extremely dense matter of neutron stars, both through tidal deformation measurements in mergers involving a neutron star and through neutron star eccentricity measures from isolated spinning neutron stars. As our detector technology improves, GWs will also allow us to perform increasingly precise tests of general relativity in regions of extreme spacetime curvature.

9. Future

We started observing with the LIGO instruments in their initial design configuration in the early 2000's and did not observe any gravitational-wave signals. The US National Science Foundation understood the need to make significant improvements in the detectors in order to achieve the required reach, and this led to the development, engineering, installation, and commissioning of the Advanced LIGO detectors – and shortly thereafter, the first observation of GWs.

The LIGO Laboratory and the LSC are now, in 2021, undertaking further modest improvements in a project named 'A+'. This project leaves in place the seismic isolation system, the quadruple suspensions, and a great deal of the electronic and optomechanical infrastructure. To the Advanced LIGO detector base, it adds 'frequency dependent light squeezing' [71] which allows us to leverage Heisenberg's Uncertainty Principle. This expresses the fact that if we make ever more precise measurements of the position, our knowledge of the speed of an object must become more uncertain. Applying this uncertainty principle to our interferometer, high light power gives us good position sensitivity at high frequencies, but shakes the optics at low frequencies, masking signals there. That trade of photon statistics versus photon pressure would normally force us to choose one or the other. Using language from quantum mechanics, we would write $\hbar = \Delta x \Delta p$, where $\hbar$ is Planck's constant, and Δx and Δp are the position and momentum (velocity times mass) of an object. If we think of Δx and Δp as vectors in 2D, we can "evade" the uncertainty principle by reducing one at the expense of the other. However, we would like to reduce Δx at high frequency and Δp at low frequency. Frequency dependent squeezing implements this. The new squeezer being prepared for A+ allows us to look with improved precision at low frequencies where the momentum transfer to the masses is a problem, and at high frequencies where the position uncertainty is determined by photon statistics.

Other changes for LIGO A+ involve replacement of mirrors with ones which have lower thermal noise in the coatings as well as less scattered light, and other changes to increase the efficiency of the optical system. The full LIGO A+ is expected to be ready to observe in 2024. Advanced Virgo is also undertaking similar improvements for 'AdV+'. The KAGRA detector in Japan is working to bring its instrument to good

sensitivity, so that we hope to have a new global network running by the early 2020's. The increase in sensitivity of the LIGO detectors will be about a factor of 2, which may sound modest; but remember that because the volume of space we explore grows as the cube of our reach, this indicates an event rate that is 2^3 or 8, which will enable a significant improvement in our studies of the populations of coalescing binaries, and provide us with new insights into the Universe.

The next step forward in the global GW network is for a third Advanced LIGO detector to come on line in India. A new LIGO-India Observatory (LIO) is starting construction in the Hingoli district in central India. This new site will contain an up-to-date LIGO detector (we produced instrumentation for three in the initial project phase), and will observe as part of an extended LIGO Laboratory. The additional detector, being far from the other detectors, will help both in the triangulation of signals and increase the fraction of time that all the instruments are operating. It is expected to begin observing in the late 2020's.

There are ambitious plans to take the field further in the 2030's. Two projects, the European Einstein Telescope (ET [72]) and the US Cosmic Explorer (CE [73]), are taking shape. In both cases, much longer arms than the current 3- and 4-km observatories are planned; the ET design envisions 10 km arms, and CE's current concept of two detectors with 20 and 40 km arms. ET has a triangular form to allow a single observatory to recover the polarization of a signal, which is important for testing the consistency of GW signals with general relativity, and is planned to be underground to reduce seismic and Newtonian noise. The two detectors for CE are optimized for the science targets. Recall that the signal size due to a given strain scales with the detector armlength. This is true for the case that the detector armlength L is short compared to the wavelength $\lambda_{GW} = c/f_{GW}$ of the gravitational wave. Once a GW wavelength is $2L$ or shorter, there are dips in sensitivity, and for for this reason a 20km antenna is optimal for observing the final phases of neutron-star merger signals at 3 to 4 kHz, and given technical limits at low frequencies for surface detectors, 40km for seeing black hole mergers at the edge of the universe [74,75]. CE is to be built on the Earth's surface, but the curvature would require a great deal of earth moving; happily, there are a number of potential sites which are 'bowls' (in fact more-or-less flat over 40km). Both of these observatories are planned to accommodate a series of improved detectors over their many-decade lifetimes; the use of cryogenics to reduce thermal noise, and evolution beyond Michelson interferometer optical systems are certainly to be included. With a sensitivity some ten times greater than today's early 2020 detectors, event rates of ten cubed – 1000 times – are anticipated, putting all of the coalescing binaries of roughly 100 solar masses in the Universe within reach (see Figure 14). Remarkable discoveries are likely to be made with the quality and quantity of data that these detectors will collect.

These new observatories will be very expensive – comparable to the biggest optical telescopes – and every effort will need to be made to make them affordable. While the technology used for the detectors themselves presents significant challenges, the biggest costs are in civil construction associated with moving earth, or tunneling, and the essential vacuum.

Just as in traditional astronomy, there is a great range of frequencies of GWs emitted by different astrophysical sources. Ground-based detectors focus on the range from $\sim$5 Hz up to a few kHz, corresponding to 'stellar' mass objects 1 to 1000 times the mass of our Sun. However, most binaries seen in telescopes coalesce in slow motion. This includes the constant hum of white dwarf binaries in our own galaxy, and distant black hole binaries so massive that the final cycles of coalescence take hours, days,

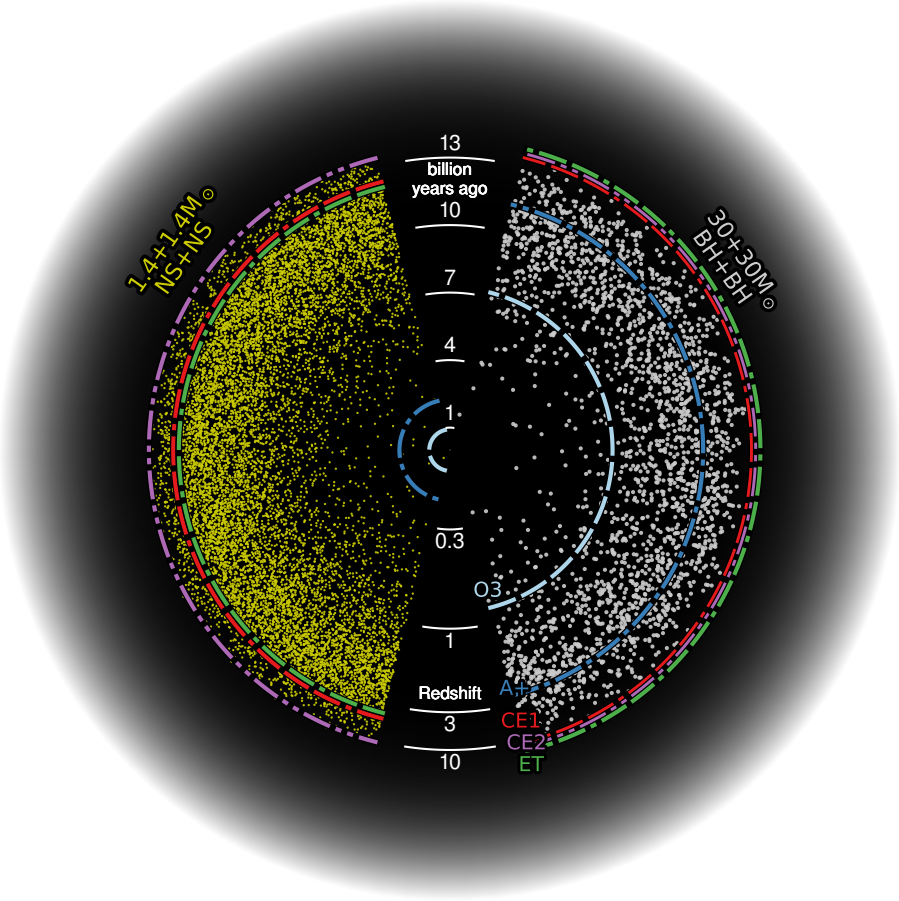

Figure 14. A visualization of the reach of generations of GW detectors. LIGO's current ('O3') and mid-2020's ('A+') sensitivity are inner rings of reach; Cosmic Explorer and Einstein Telescope extend the reach beyond the furthest and oldest coalescing compact objects in the Universe. *E. Hall, S. Vitale*

or weeks. To focus on these signals we must leave the (noisy) Earth's surface. The Laser Interferometer Space Antenna (LISA [23]) is a project using laser interferometry in space to probe the GW frequency range from around 100 microhertz to around 0.1 Hz, allowing the signals from supermassive BBHs in these coalescing galaxies to be observed. The planned arm lengths of the triangular constellation are 2.5 million km – in space, the vacuum system is free once you are there. It is a European Space Agency (ESA) led mission with significant US NASA participation, and has a planned launch date of 2034. That may seem far away, but the realities of a space mission mean that the effort is now in the early 2020's at a fever pitch [76].

At yet lower frequencies, supermassive black holes at the centers of galaxies slowly swing around each other as their host galaxies merge, distorting space-time and sending GWs throughout the Universe. To detect these sources, the International Pulsar Timing Array (IPTA [77]) uses spinning neutron stars as naturally-distributed test masses (replacing our interferometer arm mirrors) sprinkled throughout our galaxy. Mentioned above as a source of continuous-wave GW signals in the ground-based detector band, these burned-out stars act as clocks sending out highly periodic radio pulses, and a GW passing between a pulsar and the Earth will cause a phase shift in the arrival of a clock 'tick'. By simultaneously observing a number of such pulsars,

one can tease out from the noise a prescribed coherent change in pulse phase variation that must be due to GWs. This technique in the near term is likely to see a stochastic background of signals from super-massive black holes, with the best sensitivity to date already challenging some astrophysics models [78]. Future developments may allow individual sources of very low frequency GW signals to be identified.

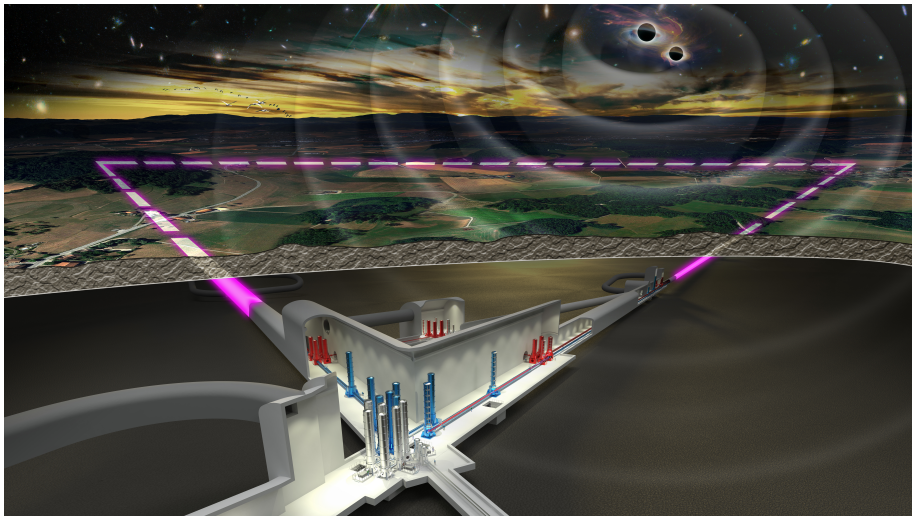

Figure 15. Conceptual diagram of the Einstein Telescope facility. Three detectors are configured in a triangular topology, and each detector consists of two interferometers. The 10 km arms of the observatory are housed underground to suppress seismic and gravity-gradient noise. Optical components are placed in an ultra-high vacuum and cryogenic environment. [72] *M. Kraan, Nikhef*

10. Conclusions

We hope we have given you a broad view of the science possible with the Advanced LIGO detectors and this new field of observational gravitational-wave astronomy. We have shown that we must overcome challenges in fundamental quantum and classical physics to observe these incredibly tiny fluctuations in spacetime generated by the dynamics of stars and black holes accelerated to near the speed of light. The required computing and precision engineering advances the state of the art on many fronts.

We can use observations from Advanced LIGO and the current detector network not only to get our first glimpse into stellar evolution across cosmic time, but also to test general relativity, inform cosmological models of the growth of large-scale structure and dark energy, and observe the interaction of matter at enormous energies inaccessible to particle accelerators on Earth.

As with any completely new method for observing the Universe, the most exciting potential source of all is the unexpected. Advanced LIGO and other gravitational wave detectors may reveal dynamic phenomena invisible to us with electromagnetic telescopes that our current understanding of physics and astronomy can't account for.

The gravitational wave discoveries to date are a testament to the power of collaborative science. In order to design, build, and commission the Advanced LIGO detectors and recover gravitational wave signals from their data, thousands of scientists, engineers, students, technicians, and staff must work together. The field's achievements would not be possible without shared effort across collaborations and continents mak-

ing the most of our resources.

This new field of gravitational wave astronomy will grow, both in the near term with continued observation by Advanced LIGO, Advanced Virgo, and KAGRA, and in the longer term with new observatories on Earth and in space. We are confident Advanced LIGO and future gravitational wave experiments will reveal more remarkable discoveries.

Acknowledgements

The authors would like to acknowledge insightful suggestions from Beverly Berger and Peter Saulson that greatly strengthened this article. The authors are grateful for computational resources provided by the LIGO Laboratory and supported by National Science Foundation Grants PHY0757058 and PHY-0823459. Most figures were produced using the publicly available PyCBC[12] and GWpy software packages[13], and public LIGO-Virgo data accessible via the Gravitational Wave Open Science Center[14]. This paper has been assigned LIGO document number LIGO-P2000530.

Funding

LIGO was constructed by the California Institute of Technology and Massachusetts Institute of Technology with funding from the National Science Foundation, and operates under Cooperative Agreement PHY-1764464. Advanced LIGO was built under Grant PHY-0823459. JM acknowledges funding from the Natural Sciences and Engineering Research Council of Canada, the Canada Foundation for Innovation, and the province of British Columbia. DHS acknowledges NSF LIGO funding, and NASA LISA funding.

About the authors

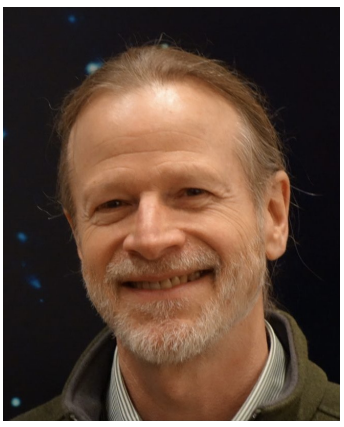


[12]PyCBC documentation and tutorials can be found here: https://pycbc.org/

[13]GWpy installation instructions, documentation, and tutorials: https://gwpy.github.io/docs/latest/

[14]There are excellent online courses, tutorials, and other resources available via the GWOSC: https://www.gw-openscience.org

Dr. David Shoemaker is a Senior Research Scientist at the Massachusetts Institute of Technology Kavli Institute. He has worked in the field of gravitational wave instrumentation since the late 1970's in Germany, France, and at MIT, and had the honor to lead the team which developed and installed the Advanced LIGO detectors. Shoemaker recently served as the Spokesperson for the LIGO Scientific Collaboration, and is currently active in LIGO and LISA.

Dr. Jess McIver is currently an assistant professor in the Department of Physics and Astronomy at the University of British Columbia. She first joined the LIGO Scientific Collaboration as an undergraduate researcher at Syracuse University working on characterization of the LIGO detectors, and expanded to GW astrophysical data analysis while she earned her PhD from the University of Massachusetts Amherst. As a postdoc with the LIGO Laboratory at Caltech, she led the effort to characterize the Advanced LIGO detectors.

References

[1] Abbott BP, Abbott R, Abbott T, et al. Observation of gravitational waves from a binary black hole merger. Physical review letters. 2016;116(6):061102.

[2] Einstein A. The collected papers of albert einstein, volume 7 (english). Princeton University Press; 2002.

[3] Web-Page. Chapel hill meeting ; 2020. Available from: `http://www.edition-open-sources.org/sources/5/index.html`.

[4] Pizzella G. Birth and initial developments of experiments with resonant detectors searching for gravitational waves. The European Physical Journal H. 2016 oct;41(4-5):267–302.

[5] Taylor JH. Pulsar timing and relativistic gravity. Classical and Quantum Gravity. 1993 dec;10(S):S167–S174.

[6] Gertsenshtein ME, Pustovoit VI. On the detection of low-frequency gravitational waves. Sov Phys JETP. 1962;:433.

[7] Moss GE, Miller LR, Forward RL. Photon-noise-limited laser transducer for gravitational antenna. Appl Opt. 1971 Nov;10(11):2495–2498. Available from: `\url{http://ao.osa.org/abstract.cfm?URI=ao-10-11-2495}`.

[8] Weiss R. Electromagnetically coupled broadband gravitational antenna, in quarterly progress report, mit research lab of electronics 105 (1972) 54. Quarterly Progress Report, MIT Research Lab of Electronics. 1972;.

[9] Danzmann K, Lück H, Rüdiger A, et al. A 600 m laser interferometric gravitational wave antenna. Gravitational Wave Experiments - Proceedings of the First Edoardo Amaldi Conference. 1995;:100.

[10] Bradaschia, Fabbro D, Virgilio D, et al. Virgo: Very wide band interferometric gravitational wave antenna. Nuclear Physics B (Proceedings Supplements). 1992;28(1):54 – 60.

[11] Whitcomb SE. The laser interferometer gravitational wave observatory (ligo) project. Classical & Quantum Gravity. 1993;10(S):1.

[12] The LIGO Scientific Collaboration, Aasi J, Abbott BP, et al. Advanced LIGO. Classical & Quantum Gravity. 2015;32(7):1.

[13] Web-Page. Ligo laboratory ; 2020. Available from: `https://www.ligo.caltech.edu/mit`.

[14] Web-Page. Virgo collaboration ; 2020. Available from: `http://public.virgo-gw.eu/the-virgo-collaboration`.

[15] Web-Page. Ligo scientific collaboration ; 2020. Available from: `https://www.ligo.org`.

[16] KAGRA Collaboration. Kagra: 2.5 generation interferometric gravitational wave detector. Nature Astronomy. 2019;3(1):35.

[17] Resnick R. Introduction to special relativity. John Wiley & Sons, Inc.; 1968. Available

from: https://www.ebook.de/de/product/3635664/robert_resnick_introduction_to_special_relativity.html.
[18] Michelson AA, Morley EW. Lviii. on the relative motion of the earth and the luminiferous æther. The London, Edinburgh, and Dublin Philosophical Magazine and Journal of Science. 1887 dec;24(151):449–463.
[19] Saulson PR. Fundamentals of interferometric gravitational wave detectors (second edition). WORLD SCIENTIFIC PUB CO INC; 2017.
[20] Fairhurst S. Localization of transient gravitational wave sources: beyond triangulation. Classical and Quantum Gravity. 2018 apr;35(10):105002.
[21] Sathyaprakash BS, Schutz BF. Physics, astrophysics and cosmology with gravitational waves. Living Reviews in Relativity. 2009 mar;12(1).
[22] Singer LP, Price LR. Rapid bayesian position reconstruction for gravitational-wave transients. Phys Rev D. 2016 Jan;93:024013. Available from: https://link.aps.org/doi/10.1103/PhysRevD.93.024013.
[23] Amaro-Seoane P, Audley H, Babak S, et al. Laser Interferometer Space Antenna ; 2017.
[24] Lommen AN. Pulsar timing for gravitational wave detection. Nature Astronomy. 2017 dec;1(12):809–811.
[25] Hobbs G, Dai S. Gravitational wave research using pulsar timing arrays. National Science Review. 2017 sep;4(5):707–717.
[26] Srivastava V, Ballmer S, Brown DA, et al. Detection prospects of core-collapse supernovae with supernova-optimized third-generation gravitational-wave detectors. Phys Rev D. 2019 Aug;100:043026. Available from: https://link.aps.org/doi/10.1103/PhysRevD.100.043026.
[27] Lorimer D. Binary and millisecond pulsars. Living Reviews in Relativity. 2008;11(8).
[28] Abbott R, Abbott TD, Abraham S, et al. Gravitational-wave constraints on the equatorial ellipticity of millisecond pulsars. The Astrophysical Journal. 2020 Oct;902(1):L21. Available from: http://dx.doi.org/10.3847/2041-8213/abb655.
[29] Abbott B, et al. A guide to ligo–virgo detector noise and extraction of transient gravitational-wave signals. Classical and Quantum Gravity. 2020;37(5).
[30] Chui C. An introduction to wavelets. Academic Press; 1992.
[31] Abbott B, et al. (LIGO Scientific Collaboration, Virgo). GWTC-1: A Gravitational-Wave Transient Catalog of Compact Binary Mergers Observed by LIGO and Virgo during the First and Second Observing Runs. Phys Rev X. 2019;9(3):031040.
[32] Klimenko S, et al. A coherent method for detection of gravitational wave bursts. Classical and Quantum Gravity. 2008;25(11).
[33] Riles K. Recent searches for continuous gravitational waves. Modern Physics Letters A. 2017;32(29).
[34] Christensen N. Stochastic gravitational wave backgrounds. Rep Prog Phys. 2018; 82(016903).
[35] Chen HY, Holz DE, Miller J, et al. Distance measures in gravitational-wave astrophysics and cosmology ; 2017.
[36] Allen B. χ^2 time-frequency discriminator for gravitational wave detection. Phys Rev D. 2005 Mar;71:062001. Available from: https://link.aps.org/doi/10.1103/PhysRevD.71.062001.
[37] Usman S, et al. The pycbc search for gravitational waves from compact binary coalescence. Classical and Quantum Gravity. 2016;33(21).
[38] Abbott B, et al. Effects of data quality vetoes on a search for compact binary coalescences in advanced ligo's first observing run. Classical and Quantum Gravity. 2018;35(065010).
[39] Reitze D, Saulson P, Grote H. Advanced interferometric gravitational-wave detectors. Singapore Hackensack, NJ: World Scientific Publishing Co. Pte. Ltd; 2019.
[40] Yu H, , McCuller L, et al. Quantum correlations between light and the kilogram-mass mirrors of LIGO. Nature. 2020 jul;583(7814):43–47.
[41] Ising G. Lxxiii. a natural limit for the sensibility of galvanometers. The London, Edinburgh, and Dublin Philosophical Magazine and Journal of Science. 1926;1(4):827–834.

[42] Heinert D, Hofmann G, Nawrodt R. Fluctuation dissipation at work: Thermal noise in reflective optical coatings for GW detectors. In: 2014 IEEE Metrology for Aerospace (MetroAeroSpace); 2014. p. 293–298.
[43] Harms J. Terrestrial gravity fluctuations. Living Reviews in Relativity. 2019;22(1):N.PAG.
[44] Web-Page. pygwinc gravitational wave interferometer noise calculator ; 2020. Available from: `https://git.ligo.org/gwinc/pygwinc`.
[45] Siegman AE. Lasers (revised). University Science Books; 1986.
[46] Yu H, McCuller L, Tse M, et al. Quantum correlations between light and the kilogram-mass mirrors of ligo. Nature. 2020;583(7814):43.
[47] Aasi J, Abbott BP, Abbott R, et al. Advanced LIGO. Classical and Quantum Gravity. 2015 mar;32(7):074001.
[48] Santini E, Teodori S. Modeling, FEM analysis and dynamic simulation of a moving coil loudspeaker. In: 2014 International Symposium on Power Electronics, Electrical Drives, Automation and Motion; 2014. p. 1306–1312.
[49] Harry G, Bodiya T, DeSalvo R. Optical coatings and thermal noise in precision measurement. Cambridge; 2012.
[50] Martynov D, Hall E, Abbott B, et al. Sensitivity of the advanced LIGO detectors at the beginning of gravitational wave astronomy. Physical Review D. 2016 jun;93(11).
[51] Weiner R. Extrapolation, interpolation, and smoothing of stationary time series. MIT Press; 1964.
[52] Davis D, et al. Improving the sensitivity of advanced ligo using noise subtraction. Classical and Quantum Gravity. 2019;36(5).
[53] Metzger B. Kilonovae. Living Reviews in Relativity. 2020;23(1).
[54] Abbott B, et al. (LIGO Scientific Collaboration, Virgo). GW170817: Observation of Gravitational Waves from a Binary Neutron Star Inspiral. Phys Rev Lett. 2017;119(16):161101.
[55] Venumadhav T, et al. New binary black hole mergers in the second observing run of advanced ligo and advanced virgo. Physical Review D. 2020;101(083030).
[56] Nitz A, et al. 2-ogc: Open gravitational-wave catalog of binary mergers from analysis of public advanced ligo and virgo data. The Astrophysical Journal. 2020;891(2).
[57] Abbott R, et al. (LIGO Scientific Collaboration, Virgo). GWTC-2: Compact Binary Coalescences Observed by LIGO and Virgo During the First Half of the Third Observing Run. Submitted to PRX. 2020;.
[58] Jonker PG, Nelemans G. The distances to galactic low-mass x-ray binaries: consequences for black hole luminosities and kicks. Monthly Notices of the Royal Astronomical Society. 2004;354(2):355–366.
[59] Abbott BP, et al. Multi-messenger observations of a binary neutron star merger. The Astrophysical Journal. 2017 oct;848(2):L12.
[60] Abbott BP, et al. A gravitational-wave standard siren measurement of the hubble constant. Nature. 2017;551:85–88.
[61] Abbott BP, et al. GW170817: Measurements of neutron star radii and equation of state. Phys Rev Lett. 2018 Oct;121:161101.
[62] Abbott BP, et al. Tests of general relativity with GW170817. Phys Rev Lett. 2019 Jul; 123:011102.
[63] Abbott BP, et al. GW190425: Observation of a compact binary coalescence with total mass $\sim$ 3.4 m $\odot$. The Astrophysical Journal. 2020 mar;892(1):L3.
[64] Abbott R, et al. GW190814: Gravitational waves from the coalescence of a 23 solar mass black hole with a 2.6 solar mass compact object. The Astrophysical Journal. 2020 jun; 896(2):L44.
[65] Abbott R, et al. GW190412: Observation of a binary-black-hole coalescence with asymmetric masses. Phys Rev D. 2020 Aug;102:043015.
[66] Abbott R, et al. GW190521: A binary black hole merger with a total mass of 150 $M_{\odot}$. Phys Rev Lett. 2020 Sep;125:101102.
[67] Abbott R, et al. Properties and astrophysical implications of the 150 m $\odot$ binary black hole merger GW190521. The Astrophysical Journal. 2020 sep;900(1):L13.

[68] Kimball C, et al. Black hole genealogy: Identifying hierarchical mergers with gravitational waves. The Astrophysical Journal. 2020;900(2).
[69] Kormendy J, Ho L. Coevolution (or not) of supermassive black holes and host galaxies. Annual Review of Astronomy and Astrophysics. 2013;51:511–653.
[70] Freedman W. Cosmology at at crossroads: Tension with the hubble constant. Nature Astronomy. 2020;0169(1).
[71] McCuller L, Whittle C, Ganapathy D, et al. Frequency-dependent squeezing for advanced LIGO. Physical Review Letters. 2020 apr;124(17).
[72] Web-Page. Einstein telescope ; 2020. Available from: http://www.et-gw.eu.
[73] Web-Page. Cosmic explorer ; 2020. Available from: https://cosmicexplorer.org.
[74] Martynov D, Miao H, Yang H, et al. Exploring the sensitivity of gravitational wave detectors to neutron star physics. Phys Rev D. 2019 May;99:102004. Available from: https://link.aps.org/doi/10.1103/PhysRevD.99.102004.
[75] Essick R, Vitale S, Evans M. Frequency-dependent responses in third generation gravitational-wave detectors. Phys Rev D. 2017 Oct;96:084004. Available from: https://link.aps.org/doi/10.1103/PhysRevD.96.084004.
[76] Web-Page. Lisa mission ; 2020. Available from: https://www.lisamission.org.
[77] Web-Page. International pulsar timing array ; 2020. Available from: http://www.ipta4gw.org.
[78] Aggarwal K, et al. The NANOGrav 11 yr Data Set: Limits on Gravitational Wave Memory. The Astrophysical Journal. 2020;889(38).